Differential Geometry and Biomolecules

Thesis. Civil Engineering.

Benny Jørgensen
(c992354)

Supervisor (main): Jens Gravesen
Department of Mathematics
Building 303

Supervisor: Henrik Bohr
Quantum Protein Centre
Building 309

The Technical University of Denmark
DK-2800 Lyngby, Denmark

December 2002

Thesis from the Technical University of Denmark.
Typeset using LyX. For more information see: www.lyx.org.

Preface

This thesis is a part of my studies at The Technical University of Denmark to become a civil engineer.

In December 2001 Director Henrik Bohr of the Quantum Protein Centre, QUP, gave a talk on biomolecules for students specialising into applied physics. After the talk I called on Henrik Bohr, and together with Associate Professor Karl Jalkanen we had discussions on subjects in the field of biomolecules and differential geometry.

In the summer of 2002 I started working on this thesis with Director Henrik Bohr as supervisor, and with Associate Professor Jens Gravesen, Department of Mathematics, as main supervisor. We had especially discussions on docking of biomolecules. One of our ideas was to use wavelets in docking programs but due to the complexity of this and lack of time we decided to concentrate on the docking program Hex.

Acknowledgements

I would like to thank Director Henrik Bohr for introducing me to the field of biomolecules, discussions and inspiration and Associate Professor Jens Gravesen for discussions and saying stop to wavelets and go with Hex; also thanks to Associate Professor Karl Jalkanen for discussions and providing me books and articles on quantum chemistry.

Also thanks to 1p and Gentofte Studenter Kursus for employment from August to December 2002.

Thanks to Associate Professor David W. Ritchie, Aberdeen University, providing me Hex during a period when the Hex homepage was down, System Administrator Tobias Mandrup Johansen, QUP, for installing Hex for me and thanks to Research Assistant Professor Morten Østergaard Jensen, QUP, for information on biomolecules and software for biochemistry.

I would also like to acknowledge Associate Professors Peter Røgen, Ole Christensen,

Michael Pedersen and Steen Markvorsen, Department of Mathematics, for various references, discussions and information.

I shall also use this opportunity to recommend the typesetting program LyX, "LaTeX with an equation editor", making life a little easier for the working mathematician.

Thanks to my friend Ph.D. Christian Tange for reading my text and giving valuable suggestions to it.

Finally thanks to Bjørn, Vibeke, Salim, Haim and Mai at QUP for discussions and being there and thanks to the friendly staff at the reception at the Department of Mathematics.

December 30, 2002

Benny Jørgensen

Summary

The title of this thesis is Differential Geometry and Biomolecules. Within the range of this title my work can be divided into three:

- Solvent effects. The biomolecule in a dielectric cavity.
- Biomembranes.
- Docking programs.

A large part of my work has been to search the scientific literature and the Internet for relevant and up to date information about these three subject. References to books, articles and Internet sites are given in the bibliography at the end of the thesis; a reference is shown in square brackets: [ ].

My investigations on solvent effects was after considerations together with Karl Jalkanen. Was it possible to treat other cavities than spherical and ellipsoidal? Searching the literature and the internet I found a new article [Cossi et al, 02] giving a positive answer to this question. This answer was also confirmed in a talk given by Per Siegbahn November 7, 2002, at QUP. In the thesis I try to give some information about the present state of quantum chemistry and solvent effects but I do not go into details.

Biomembranes was a subject I heard about from Henrik Bohr. I found a monograph [Ou-Yang et al, 99] on the subject and in the thesis I try to give the reader an idea of how biomembranes can be treated mathematically. True classical differential geometry is used.

The largest part of this thesis is devoted to the subject of docking programs which I worked on together with Henrik Bohr and Jens Gravesen. We knew that Michael Connolly had made a program which could generate molecular surfaces with pdb-files as input (pdb: protein database). Basicly starting from Connolly's webpage and searching the Internet and the literature I ended up with an invited review article [Halperin et al, 02] from June this year on docking programs. I give some information about this review article and different docking programs and then I in detail consider David W. Ritchie's docking program Hex. In the rigid-body approximation docking programs give an answer to the problem of how to *computationally find the best fit between two surfaces.*

Contents

Part I

The Solvent, Biomembranes and Docking Programs

Chapter 1

Biomolecules

We shall not investigate the large knowledge of structures of biomolecules. This is not within the scope of this thesis. But for own and maybe some readers convenience we review a few basic principles.

Every day we see information of the amount of energy-providing proteins, carbohydrates or lipids (fat) on the back of the packing of our food. Fundamentally these biomolecules together with the nucleic acids (DNA, RNA) (or some of their smaller building blocks) are participants in all lifeprocesses. Our main concern are proteins which are formed from peptides which again are made up of amino acids. References are [Jakubke & Jeschkeit, 82], [Schulz & Schirmer, 79], [Branden & Tooze, 99] and [Stryer, 88].

Proteins play important roles in different settings ([Stryer, 88] page 15):

1. Enzymatic catalysis. Enzymes catalyse chemical reactions in biological systems. Nearly all enzymes are proteins.

2. Transport and storage. Many small molecules and ions are transported by specific proteins.

3. Coordinated motion. On the scale of muscles two kinds of protein filaments slide against each other under the action of muscle contraction. On the microscopic scale, as an example, the movement of chromosomes in mitosis are produced by contractile assemblies of proteins.

4. Mechanical support. The strength of skin and bone is due to the presence of collagen, a fibrous protein.

5. Immune protection. Antibodies are highly specific proteins.

6. Generation and transmission of nerve impulses. Receptor proteins mediate specific stimuli.

7. Control of growth and differentiation. For example, many hormones are proteins.

Biomembranes are of our concern too. The cell membrane are the necessary interface between the cell and its environment. An example of a biomembrane is the membrane of the human red blood cell, which is easier to study than the most membranes due to the lacking nucleus of the human red blood cell. The reference is here [Ou-Yang et al, 99].

1.1 Amino Acids

Amino acids have to our knowledge existed on the planet Earth for more than three billion (10^9) years. The existence of amino acids outside the Earth system is verified too ([Jakubke & Jeschkeit, 82] page 13).

Most of the multitude of physics and chemistry of amino acids are due to the coexistence of the basic amino group NH_2- and the acid carboxyl group $-COOH$. Amino acids are made up from these two groups, a side chain R, a hydrogen atom H and a carbon atom, the C_α-atom:

$$\begin{array}{ccccc} & & R & & \\ & & | & & \\ H-N- & & C_\alpha & -C'-OH & \\ & | & | & || & \\ & H & H & O & \end{array}$$

Looking from the hydrogen atom along the $H-C_\alpha$ bond and remembering the more or less tetrahedral structure we see, that there are two geometrical forms of the amino acids or two chiral forms, the L-form and the D-form (not all atoms are shown):

L-form

$$\begin{array}{ccccc} & & R & & \\ & & | & & \\ & & C_\alpha & & \\ & / & | & \backslash & \\ CO & & H & & N \end{array}$$

D-form

$$\begin{array}{ccccc} & & R & & \\ & & | & & \\ & & C_\alpha & & \\ & / & | & \backslash & \\ N & & H & & CO \end{array}$$

In biological systems in nature (as an evolutionary fact) the L-form of the amino acids is chosen.

Peptides are build from amino acids connected through *peptide bonds* between the N (nitrogen) and the C' (carbon) atoms:

$$\begin{array}{ccccccccc} & & R_1 & & & & H & H & \\ & & | & & & & | & | & \\ -N- & & C_\alpha & & -C'- & N & - & C_\alpha & -C'- \\ | & & | & & || & & & | & \\ H & & H & & O & & & R_2 & \end{array}$$

Twenty different amino acids are present in proteins. The most simple is *glycine*, abbreviated Gly or G, where the side chain R just is hydrogen H.

Glycine

$$\begin{array}{ccccc} & & H & & \\ & & | & & \\ H-N- & & C_\alpha & -C'-OH & \\ & | & | & || & \\ & H & H & O & \end{array}$$

Seven of the twenty amino acids are *hydrophobic* (non-polar):

Name	Three-letter code	One-letter code	Name of discoverer
Alanin	Ala	A	Weyl (1888)
Valin	Val	V	Gorup-Besanez (1856)
Phenylalanine	Phe	F	Schulze and Barbieri (1879)
Proline	Pro	P	Fischer (1901)
Methionine	Met	M	Mueller (1921)
Isoleucine	Ile	I	Ehrlich (1904)
Leucine	Leu	L	Proust (1819)

We now list a kind of structure formula for the above amino acids. Excuse the clumsy typing; but the meaning should come through. For alanin the whole structure is shown, but for the rest *only the side chains* R are shown.

Alanin

$$\begin{array}{ccccc} & & CH_3 & & \\ & & | & & \\ H_3N^+- & & C & -COO^- & \\ & & | & & \\ & & H & & \end{array}$$

Valine

$$\begin{array}{ccc} H_3C & & CH_3 \\ \quad\backslash & & /\quad \\ & CH & \\ & | & \end{array}$$

Phenylalanine

$$\begin{array}{lll} HC & -CH= & CH \\ \| & & | \\ HC & -C= & CH \\ & | & \\ & CH_2 & \\ & | & \end{array}$$

Proline

$$\begin{array}{lll} CH_2 & - & CH_2 \\ \quad/ & & \quad\backslash \\ CH_2 & & C_\alpha H \\ \quad\backslash & & \quad/ \\ & N & \\ & | & \end{array}$$

Methione

$$CH_3 - S - CH_2 - CH_2 -$$

Isoleucine

$$\begin{array}{ccc} CH_3 & & \\ | & & \\ H_2C & & CH_3 \\ \quad\backslash & & /\quad \\ & CH & \\ & | & \end{array}$$

Leucine

$$\begin{array}{ccc} H_3C & & CH_3 \\ \quad\backslash & & /\quad \\ & CH & \\ & | & \end{array}$$

Four of the twenty amino acids are *charged*:

Name	Three-letter code	One-letter code	Name of discoverer
Aspartic acid	Asp	D	Ritthausen (1868)
Glutamic acid	Glu	E	Ritthausen (1866)
Lysine	Lys	K	Drechsel (1899)
Arginine	Arg	R	Schulze et al (1886)

Again we list chemical formulas for the side chains of these four amino acids.
Aspartic acid

$$\begin{array}{cc} O & =C- \quad O^- \\ & | \\ & CH_2 \\ & | \end{array}$$

Glutamic acid

$$\begin{array}{cc} O & =C- \quad O^- \\ & | \\ & CH_2 \\ & | \\ & CH_2 \\ & | \end{array}$$

Lysine

$$NH_3^+ - CH_2 - CH_2 - CH_2 - CH_2-$$

Arginine

$$\begin{array}{ccc} & NH_2^+ & \\ & || & \\ NH_2- & C & -NH - CH_2 - CH_2 - CH_2- \end{array}$$

The last eight amino acids are *polar*:

Name	Three-letter code	One-letter code	Name of discoverer
Serine	Ser	S	Cramer (1865)
Threonine	Thr	T	Rose et al (1935)
Tyrosine	Tyr	Y	Liebig (1846)
Histidine	His	H	Kossel (1896)
Cysteine	Cys	C	Baumann (1884)
Asparagine	Asn	N	Vauquelin and Robiquet (1806)
Glutamine	Gln	Q	Schulze (1877)
Tryptophan	Trp	W	Hopkins and Cole (1901)

We give the chemical formulas for the side chains.

Serine

$$HO - CH_2 -$$

Threonine

$$\begin{array}{l} HO \quad -CH- \quad CH_3 \\ \qquad\quad | \end{array}$$

Tyrosine

$$HO - (C_6H_4) - CH_2 -$$

Histidine

$$(C_3N_2H_3) - CH_2 -$$

Cysteine

$$HS - CH_2 -$$

Asparagine

$$\begin{array}{l} O \quad = C - \quad NH_2 \\ \qquad\quad | \\ \qquad CH_2 \\ \qquad\quad | \end{array}$$

Glutamine

$$\begin{array}{l} O \quad = C - \quad NH_2 \\ \qquad\quad | \\ \qquad CH_2 \\ \qquad\quad | \\ \qquad CH_2 \\ \qquad\quad | \end{array}$$

Tryptophan

$$(C_8NH_6) - CH_2-$$

1.2 Peptides

Amino acids are joined together through *peptide bonds* between the carbon C' and the nitrogen N atom. *Peptides* or polypeptides are the resulting molecules after joining several amino acids together through peptide bonds. The $C' - N$ distance in peptides is shorter than a normal $C - N$ single-bond distance ([Jakubke & Jeschkeit, 82] page 96). Most of the peptides are linear chains without connected ends, but also peptides with connected ends, cyclic peptides, exist.

The biochemist's way of dividing the peptides is at the peptide bond between the C' and the N atoms as explained earlier:

$$\begin{array}{cccccccccc} & & R_1 & & & & H & H & & \\ & & | & & & & | & | & & \\ -N- & & C_\alpha & & -C'- & N & - & C_\alpha & - & C'- \\ | & & | & & || & & & | & & \\ H & & H & & O & & & R_2 & & \end{array}$$

Another approach, the structural, is the following. The covalent bonds in the units from one C_α atom to the next C_α atom are very rigid and these units can be viewed as small planes:

$$\begin{array}{cccccccccc} R_1 & & & & H & O & H & & R_3 & \\ | & & & & | & || & | & & | & \\ -C_\alpha & -C'- & N & - & C_\alpha & - & C'- & N- & C_\alpha & - \\ | & || & | & & | & & & & | & \\ H & O & H & & R_2 & & & & H & \end{array}$$

Each C_α atom belongs to two of these units (except the first and last C_α atom in the linear peptide). The side chains and the hydrogen atom bound to the C_α atom are not part of these units. The units can rotate around two bonds; the $N - C_\alpha$ bond with angle denoted ϕ (phi) and the $C_\alpha - C'$ bond with angle denoted ψ (psi). In a *Ramachandran plot* these two angles are plotted against each other. Due to the finiteness in volume of the side chains (R) and the "main chain" or "back bone" ($-C_\alpha - C' - N - C_\alpha - C' - N-$) not every value of the (ϕ, ψ)-pair is possible and important information can be gained from specific Ramachandran plots.

1.3 Proteins

Proteins consist of one or more polypeptides, that is amino acid sequences, and are conveniently described on four levels, the *primary*, *secondary*, *tertiary* and *quarternary structures*.

The primary structure is the amino acid sequence. The sequences have been found for very many proteins and the number is increasing rapidly. Of course the sequence is a key in understanding the protein, but as a comparison, the often posed question is ([Branden & Tooze, 99] page 3), how much information do one get from a telephone directory about the life in a city? The polypeptides can evolve into regular geometries such as α-helices or β-strands (we will not discuss these forms at this place). Identifying the secondary structure of a protein is to identify the different parts of the sequence with such structure. The tertiary structure is the structure formed by three-dimensional packing of the secondary structure into one or several units called domains. The quarternary structure is what makes up the final protein; it can contain several polypeptides and amino acids far apart in the sequence can meet and form an *active site*. The polypeptides are as the above shows folded into each other in a complicated way. The *problem of folding*, that is going from the sequence to the final protein, is still unsolved.

Formation of secondary structure and folding is mediated through *non-covalent forces*. These can be divided into the following four types ([Schulz & Schirmer, 79] page 44):

- Repulsion between nonbonded electron shells
- Attractive coupling between oscillating dipoles
- Electrostatic attraction and repulsion of partial charges as well as attraction of full charges as found in salt bridges
- Hydrogen bonds

An important fact one always should remember is that real proteins are in solution and the effect of the solvent system must be taken into account.

1.4 DNA and RNA

DNA, deoxyribonucleic acid, has a sugar-phosphate double backbone with four types of nitrogenous bases connected to the backbone. The four bases are adenine (A), guanine (G), thymine (T) and cytosine (C).

In RNA, ribonucleic acid, the sugar units are riboses whereas they are deoxyriboses in DNA. Additionally in RNA the base uracil (U) is present instead of thymine (T).

The flow of genetic information in normal cells is the following ([Stryer, 88] page 91):

$$DNA \xrightarrow{transcription} RNA \xrightarrow{translation} Protein$$

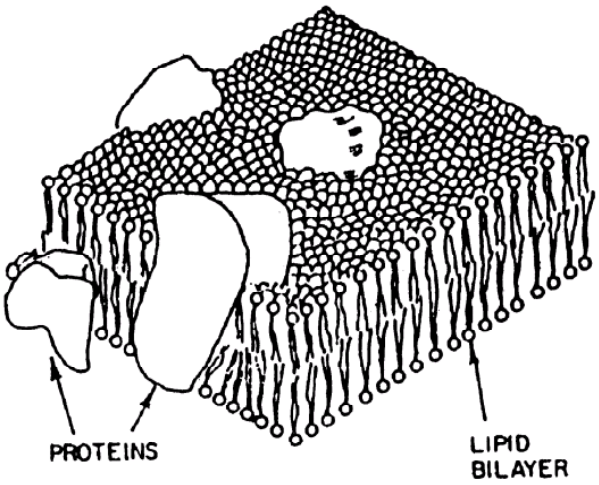

Figure 1.1: [Ou-Yang et al, 99] page 14. The fluid mosaic model of biomembranes.

A sequence of three bases, called a codon, specifies an amino acid. The codons UAA, UAG and UGA are signals for chain termination. Since $4^3 = 64$ there are 61 codons for the 20 amino acids and therefore more than one codon for most amino acids.

1.5 Biomembranes

The accepted picture of biomembranes is the *fluid mosaic* model proposed by Singer and Nicholson in 1972 ([Ou-Yang et al, 99] page 13).

In this model the membrane consists of a bilayer of amphiphilic lipids with embedded protein and enzyme molecules. The proteins and enzymes mediate between the interior and the outside of the cell. The amphiphilic lipids can move freely in the membrane surface like ordinary liquid molecules. Also the proteins and enzymes are allowed to move.

Amphiphilic molecules (from greek, amphi: on both sides) are able to form homogeneous solutions with both water or other polar solvents as well as oil or other nonpolar solvents. Amphiphilic molecules have both a polar part and a nonpolar part.

Biomembranes contain amphipilic bio-lipids with two hydrocarbon chains (the nonpolar and hydrophobic part) and a single polar and hydrophilic head. Many of these bio-lipids are phosphoglycerides which have the following general formula ([Ou-Yang et al, 99] page 15):

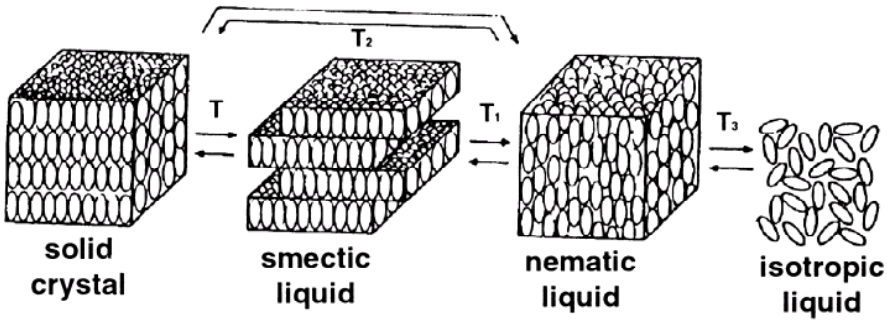

Figure 1.2: [Ou-Yang et al, 99] page 2. Two liquid crystal states.

$$
\begin{array}{lll}
 & & O^- \\
 & & | \\
CH_2 & -CH- & CH_2 - O - P - O - X \\
| & | & || \\
O & O & O \\
| & | & \\
O = C & C = O & \\
| & | & \\
R_1 & R_2 &
\end{array}
$$

where R_1 and R_2 are hydrocarbon chains and X is the polar head group. With hydrocarbon chains of normal length (about 10 carbon atoms) the bio-lipids mostly form bilayer structure in water.

Cell membranes are complicated structures with a lot of different bio-lipids, cytoskeleton, cholesterol and other biomolecules. The amount of cholesterol in the phospholipid bilayer may reach the level of one cholesterol molecule to one phospholipid molecule ([Ou-Yang et al, 99] page 15). The chemical and biological effects of cholesterol in biomembranes are not understood very well; a phenomenon is that a high amount of cholesterol can ultimately eliminate a (temperature - heat flow rate) phase transition.

Some agregates of molecules can beside the usual three states of phase: solid, liquid and gaseous, exist in an intermediate state between the solid and the liquid phase: the liquid crystal phase. The similarity between smectic liquid crystals and fluid membranes (such as biomembranes) made W. Helfrich in 1973 come up with an elastic theory of membranes.

Liquid crystals are characterized through a high degree of directional order. Today liquid crystals are used in the display of pocket calculators (LCD: liquid crystal display) and used in computerscreens. It is interesting that the input to some succes in explaining the behaviour of the shape of biomembranes was the similarity with liquid crystals.

Chapter 2

Many-Body Schrödinger Operators

The fundamental physics describing biomolecules on the smallest reasonable scale is well known: *it is quantum physics*. Non-relativistic quantum physics with relativistic corrections do describe atoms very well. Non-relativistic quantum physics originates in the work of Schrödinger and Heisenberg in the years 1925-1926. The wave mechanics formulation of Schrödinger is now the most used. Dirac came with his relativistic quantum theory a short time later and relativistic corrrections to the Schrödinger equation arise from this theory. John A. Pople could in his 1998 Nobel Lecture [Pople, 99], *Quantum chemical models*, state that: "*...no significant failure of the full Schrödinger-Dirac treatment has ever been demonstrated.*"

We shall comment a little on the present state of quantum chemistry, assuming the reader has some basic knowledge, and give W. Kohn's [Kohn, 99] rough explanation from his 1998 Nobel Lecture, *Electronic structure of matter - wave functions and density functionals*, of why ab initio quantum chemical computations only are of restricted use for large biomolecules - the computations are too demanding.

2.1 Many-Body Schrödinger Operators

The time-dependent Schrödinger equation is:

$$i\hbar\frac{\partial\psi}{\partial t} = H\psi$$

where H is the Schrödinger operator. H is a differential operator and $\psi(\mathbf{x}, t)$ is the wavefunction. The square of the norm of the wavefunction, $|\psi(\mathbf{x}, t)|^2$, is proportional to the probability density function describing the positions or configuration of the particles at the time t. In writing $\psi(\mathbf{x}, t)$ we have let the wavefunction depend on positions $\mathbf{x}$ and time t suppresing spin-variables. The time-independent Schrödinger equation is the eigenvalue problem: $H\psi = E\psi$, where E is the energy of the system. In most cases is it the time-independent Schrödinger equation which is studied.

For a system of N electrons and nuclei the many-body Schrödinger operator takes the form:

$$H = H_o + V = \sum_{i=1}^{N} -\frac{\hbar^2}{2m_i}\Delta_i + \sum_{i<j}^{N} \frac{k_c q_i q_j}{|x_i - x_j|} \,.$$

$H_o = \sum_{i=1}^{N} -\frac{\hbar^2}{2m_i}\Delta_i$ is the operator describing the free motion or kinetic energy of the particles (Δ denotes the Laplacian operator) and $V = \sum_{i<j}^{N} \frac{k_c q_i q_j}{|x_i - x_j|}$ is the multiplication operator describing the Coulomb interaction or potential energy of the particles. Notice, that the Coulomb interaction is *long range*, it decays as $\frac{1}{r}$, r being the distance between two particles. External electric field (the Stark effect) and external magnetic field (the Zeeman or Paschen-Back effect) give rise to additional terms in the potential. This is also the way to include relativistic corrections.

In the *Born-Oppenheimer approximation* the nuclei (which are much heavier than the electrons) are considered to be at rest at positions x_l and the Schrödinger operator for the many-electron system becomes:

$$H = \sum_{k} -\frac{\hbar^2}{2m}\Delta_k + \sum_{k,l} -\frac{Z_l e^2}{|x_k - x_l|} + \sum_{k<k'} \frac{e^2}{|x_k - x_{k'}|} \,.$$

Here Z_l is the atomic number of the nuclei and $\hbar$, m and e are fundamental constants (units are chosen so that k_c equals one). In the Schrödinger equation the wavefunction ψ is now considered as a function of the electron positions x_k only. Solving the time-independent Schrödinger equation analytically has only been done for hydrogen and hydrogen-like ions, therefore one has to resort to numerical solution; but even this is a very difficult task.

2.2 Calculation of Wavefunctions

According to John A. Pople [Pople, 99] there have been essentially two ways of getting reasonable accurate results (about 1 kcal/mole) for larger and larger many-electron systems. First using larger basis sets made possible through the development in accessible computer hardware was and will be a main strategy. Second different methods for taking electron correlation into account was developed and is also open for further development in the future. A number of 50 electrons was in 1998 not far away ([Pople, 99] page 1273) maybe corresponding to about 10 atoms ([Kohn, 99] page 1265). One can always use more computational force but to the authors knowledge these numbers more or less are the state of the art at a reasonable runtime today. For larger systems one can do density functional calculations but this gives a smaller amount of information than solution of the Schrödinger equation.

A common package today for these calculations is the Gaussian package [Gaussian], which have had many updates. John A. Pople and his group began the development of the Gaussian package in 1968. The name of the package refers to the use of Gaussian-type functions in the basis. Already in 1950 it had been shown that all integrals in self-

consistent field theory could be evaluated analytically if the radial parts had the form $P(x,y,z)exp(-r^2)$, where P is any polynomial in x, y and z ([Pople, 99] page 1269).

W. Kohn gives ([Kohn, 99] page 1257) some kind of explanation of the hardness of numerical solution of the Schrödinger equation. The ground state energy can be calculated minimizing the expectation value of the energy: $< \psi, H\psi >= \int \psi^*(\mathbf{x}) H\psi(\mathbf{x}) d\mathbf{x}$. A common way to minimize this value is to let the wavefunction depend on parameters $p_1, ..., p_M$ and minimize $< \psi, H\psi >$ as a function of these parameters. Kohn *guesses* that there must be p parameters for every one-dimensional continuous variable and $3 \leq p \leq 10$. Further he *guesses* that the number of parameters M depends in the following way on p and the number N of electrons: $M = p^{3N}$. There is no exact justification for this crucial ansatz. Optimistically assuming that with the best available computer software and hardware M is 10^9 and also $p = 3$ he gets $N = \frac{1}{3}\frac{\ln M}{\ln p} = 6$; a very small number! Kohn says the many-electron system encounters an *exponential wall*. Of course another relationship between M, p and N will give another result and in practice (Kohn says by being "clever") one can do better than just 6. It is necessary to be careful with an estimate of this type but still it maybe shows something about the hardness of the problem.

2.3 Density Functional Theory

In density functional theory the main quantity is the electron density function $\rho(x)$ defined as:

$$\rho(x) = N \cdot \int \psi^*(x, x_2, x_3, ..., x_N)\psi(x, x_2, x_3, ..., x_N)\, dx_2 dx_3 ....dx_N \ .$$

Here ψ is shown as a function of the electron positions x_i (we are not showing the spin-variables) and therefore antisymmetric when interchanging two variables leaving ρ independent of the above position of x in ψ; remember electrons are indistinguishable particles or *fermions* corresponding to antisymmetric wavefunctions.

The electronic ground state energy E can in density functional theory be calculated as a functional of ρ: $E = E(\rho)$. It can be done with a significantly lower computational cost at a reasonable accuracy than solution of the Schrödinger equation. Density functional theory is therefore well suited for larger systems and the state of the art in 1998 was systems of the order of 100 to 1000 atoms ([Kohn, 99] page 1254). It is possible to obtain information about other things than the ground state energy but in general not as much as from a solution of the Schrödinger equation; for instance excited states are hard to treat in density functional theory: without wavefunctions the orthogonality of excited states and the ground state is not an easy task to ensure ([Jensen, 98] page 189).

2.4 Non-Quantum Approaches

Owing to the high computational cost in a full quantum treatment of a protein or other biomolecules one often resorts to solve Newton's second law with different empirical po-

tentials (also called *force fields*) describing the interactions between the atoms; in the literature this is denoted *molecular mechanics* or *molecular dynamics*.

A way to treat a protein is to do molecular mechanics for the protein or the interesting part of the protein as a whole and do quantum calculations at the active site of the protein.

An older software program for molecular dynamics is *CHARMM* [Brooks et al, 83]. A more modern parallel, object-oriented molecular dynamics code is *NAMD*. NAMD is file-compatible with for instance CHARMM. For visualization a program such as *VMD* could be used. Many other software programs for computational chemistry exist [antas].

2.5 Treatment of the Solvent

Most biological processes take place in solution. It is of course not possible to solve the full Schrödinger equation for a biomolecule and all the molecules in the solvent. What one does is to make a kind of *shell-model* of the system.

In this shell-model the biomolecule is at the center. Around the biomolecule in a shell is maybe a few water-molecules or some other molecules of the solvent. If these two parts of the system are small enough they could be treated as a quantum system, otherwise one would use molecular dynamics.

In the next shell one usually has a large amount of molecules from the solvent; *the discrete approach*. These molecules can be treated in two ways ([Jensen, 98] page 376). Either one uses molecular dynamics or a *Monte Carlo* (stochastic) method. The Monte Carlo methods exploit the Boltzmann factor $e^{-\Delta E/k_B T}$ to find the positions of the molecules of the solvent in phase space (position and linear momentum).

In the outmost shell one considers the solvent as a continous dielectric medium; *the continous approach*. The medium is polarized with impact on the chemical characteristics of the system.

Of course in practical applications one does not necessarily use all of the above shells or one has some extra features.

The use of a continous dielectric medium around the biomolecule at the center has its origin in the Onsager model ([Foresman et al, 96], [Onsager, 36]). In the Onsager model the biomolecule is placed in a spherical or ellipsoidal cavity. It is remarkable that ***it is possible to use realistic shapes of the cavity*** and not only spherical or ellipsoidal cavities with a complete solution of the electrostatic problem; see [Cossi et al, 02]. A feature article on the discrete approach is: [Gordon et al, 01]. In [Bandyopadhyay, 02] one can see how it is possible to combine the discrete and the continous approach.

Chapter 3

Differential Geometry

When comparing textbooks on applied differential geometry in physics, for example in the area of general relativity, with modern textbooks on advanced mathematical differential geometry it looks like two different worlds. Cut to the bone this is not the case and the best is of course, if possible, to comprehend both approaches. Maybe one can say that the more modern mathematical advanced approach is suited to the global properties whereas the applied mathematical physics approach is local. In [Ou-Yang et al, 99] the approach is the classical applied. A new textbook trying to fill the gap between older textbooks and modern mathematical textbooks on differential geometry is [Talpaert, 01].

To get the approach in [Ou-Yang et al, 99] in the right perspective we very shortly give some information on a few differential geometric tools. It will primarily be using the classical local coordinate approach for which chapter 7 and 8 in [Spiegel, 59] is a good straightforward outline. For more detailed information consult the references or textbooks on differential geometry.

3.1 Curvilinear Coordinates

We all know examples of curvilinear coordinates, it could be cylindrical coordinates or spherical coordinates, you name it. The rectangular coordinates (x, y, z) of any point P is expressed as functions of (u_1, u_2, u_3) so that

$$x = x(u_1, u_2, u_3)\,, \quad y = y(u_1, u_2, u_3)\,, \quad z = z(u_1, u_2, u_3)\,.$$

Suppose that these equations can be solved for u_1, u_2, u_3 in terms of x, y, z, that is,

$$u_1 = u_1(x, y, z)\,, \quad u_2 = u_2(x, y, z)\,, \quad u_3 = u_3(x, y, z)\,.$$

These six functions must satisfy certain regularity conditions. In practice certain points may need special treatment. The unique set of coordinates (u_1, u_2, u_3) are called the *curvilinear coordinates* of P. The important notion of *orthogonal* curvilinear coordinates is introduced in an obvious way.

Let $\mathbf{r} = x\mathbf{i} + y\mathbf{j} + z\mathbf{k}$ be the position vector of a point P. Then we can write $\mathbf{r} = \mathbf{r}(u_1, u_2, u_3)$. A tangent vector to the u_1 curve at P (for which u_2 and u_3 are constants) is $\frac{\partial \mathbf{r}}{\partial u_1}$, and in the same way are $\frac{\partial \mathbf{r}}{\partial u_2}$ and $\frac{\partial \mathbf{r}}{\partial u_3}$ tangent vectors to the u_2 and u_3 curves respectively at P.

The vector ∇u_1 is a vector at P normal to the coordinate surface $\mathrm{u}_1 = c_1$, and in the same way are ∇u_2 and ∇u_3 vectors at P normal to the coordinate surfaces $\mathrm{u}_2 = c_2$ and $u_3 = c_3$ respectively.

A vector $\mathbf{A}$ at P can now be expressed in two ways. We can write

$$\mathbf{A} = C_1 \frac{\partial \mathbf{r}}{\partial u_1} + C_2 \frac{\partial \mathbf{r}}{\partial u_2} + C_3 \frac{\partial \mathbf{r}}{\partial u_3}\,,$$

and

$$\mathbf{A} = c_1 \nabla u_1 + c_2 \nabla u_2 + c_3 \nabla u_3\,.$$

C_1, C_2, C_3 are called the *contravariant components* of $\mathbf{A}$ and c_1, c_2, c_3 are called the *covariant components* of $\mathbf{A}$. Note that a vector $\mathbf{A}$ is a quantity independent of the choice of coordinate system, just like real physical quantities; this is called *invariance*, which is an important idea in what follows. One can show that if (u_1, u_2, u_3) and $(\overline{u}_1, \overline{u}_2, \overline{u}_3)$ are two general curvilinear coordinate systems then the corresponding contravariant components of $\mathbf{A}$ transform the following way

$$C_p = \sum_{q=1}^{3} \overline{C}_q \frac{\partial u_p}{\partial \overline{u}_q}\,, \qquad p = 1, 2, 3\,, \tag{3.1}$$

and the covariant components transform this way

$$c_p = \sum_{q=1}^{3} \overline{c}_q \frac{\partial \overline{u}_q}{\partial u_p}\,, \qquad p = 1, 2, 3\,. \tag{3.2}$$

3.2 Tensors

If three quantities C_1, C_2, C_3 of a coordinate system (u_1, u_2, u_3) transform as in the result (3.1), the quantities are called *components of a contravariant vector* or a *contravariant tensor of the first rank*. If three quantities c_1, c_2, c_3 of a coordinate system (u_1, u_2, u_3) transform as in the result (3.2), the quantities are called *components of a covariant vector* or a *covariant tensor of the first rank*.

This definition of contravariant tensors and covariant tensors of the first rank is generalized in tensor analysis where multiple quantities (contravariant, covariant and mixed tensors) transforming according to generalizations of (3.1) and (3.2) are treated. *Superscripts* indicate contravariant components and *subscripts* indicate covariant components; an exception occurs in the notation for coordinates (usually superscripts are used).

Different operations such as addition of tensors of the same type and other operations can easily be defined.

Tensors can be differentiated to become new tensors, but in general this is not just a partial differentiation with respect to a coordinate. One has to introduce the socalled *Christoffel's symbols*, which not are tensors, to make the differentiation feasible and the differentiation is the one of *covariant differentiation*.

In general the space considered is not just three dimensional but N dimensional with coordinates $(x^1, x^2, ..., x^N)$. Maybe the most important link to the geometric situation is the *line element* ds given by the quadratic form, called the *metric form* or *metric*, using the *metric tensor* g_{pq}. Using Einstein's summation convention (summation over repeated indices) the line element is given through the relation

$$ds^2 = g_{pq} dx^p dx^q \, .$$

If the metric tensor exists the space is called *Riemannian*. More precisely if the metric form is positive definit (ds^2 is zero for $dx^p = 0$ and positive otherwise) the space is *Riemannian*, if not (ds^2 can be zero or negative for nonzero dx^p) it is a *pseudo-Riemannian* space. In general relativity the four dimensional space-time continuum is a pseudo-Riemannian space and the metric tensor do appear in the Einstein field equations.

3.3 Surfaces

In [Ou-Yang et al, 99] they of course consider biomembranes as two dimensional surfaces in the usual three dimensional *Euclidean* space. As mathematical objects such surfaces inherit a lot of structure from the Euclidean space, for example a metric. We can represent the surface through a mapping $\mathbf{r}(u_1, u_2)$, $(u_1, u_2) \in D$. Then

$$d\mathbf{r} = \frac{\partial \mathbf{r}}{\partial u_1} du_1 + \frac{\partial \mathbf{r}}{\partial u_2} du_2.$$

Note that the vectors $\frac{\partial \mathbf{r}}{\partial u_p}$, $p = 1, 2$, span the tangent plane at $\mathbf{r}$. Now

$$ds^2 = d\mathbf{r} \cdot d\mathbf{r} = (\frac{\partial \mathbf{r}}{\partial u_1} du_1 + \frac{\partial \mathbf{r}}{\partial u_2} du_2) \cdot (\frac{\partial \mathbf{r}}{\partial u_1} du_1 + \frac{\partial \mathbf{r}}{\partial u_2} du_2)$$

so

$$ds^2 = \sum_{p=1}^{2} \sum_{q=1}^{2} g_{pq} du_p du_q \, , \quad g_{pq} = \frac{\partial \mathbf{r}}{\partial u_p} \cdot \frac{\partial \mathbf{r}}{\partial u_q}. \tag{3.3}$$

It is interesting to note that in the context of surfaces of two dimensional surfaces embedded in a three dimensional Euclidean space a *covariant derivative* ([Do Carmo, 76] page 238) of a differentiable vector field can be defined by means of projection onto the tangent plane together with other notions.

It is important to note that in general it is not possible to cover a surface in a differentiable way just using one mapping $\mathbf{r}(u_1, u_2)$, $(u_1, u_2) \in D$, one needs more functions, also called *charts*; this is the beginning of the theory of *manifolds*.

Chapter 4

Biomembranes

We will have a look at how they study biomembranes in [Ou-Yang et al, 99]. In 1973 W. Helfrich proposed in analogy with smectic-A liquid crystal bilayers that the *shape energy* of a vesicle is given by:

$$F = \frac{k_c}{2} \cdot \int (2H + c_o)^2 dA + (p_{out} - p_{in}) \cdot \int dV + \lambda \cdot \int dA \,. \tag{4.1}$$

The first and the last integral on the right hand side are surface-integrals over the surface of the vesicle whereas the second integral is a volume-integral over the vesicle.

$\frac{k_c}{2} \cdot \int (2H + c_o)^2 dA$ is the curvature-elastic energy of the vesicle membrane. Here k_c is the bending rigidity of the membrane, H is the mean curvature of the membrane surface and c_o is the spontaneous curvature of the surface. Both H and c_o are functions on the surface. The spontaneous curvature c_o takes acount of asymmetry effects of the membrane or its environment; in applications it often is considered as a constant. The difference $p_{out} - p_{in}$ is the pressure difference between the outside and the inside of the membrane and λ is the tensile stress acting on the membrane.

As a general principle of nature systems seek towards states of minimum energy and in equilibrium the energy of the system will be at a (local) minimum. If the shape energy of a vesicle is at a minimum the "first variation" of the shape energy through changing the shape of the membrane surface must be zero. First variation of the shape energy F leads to the *general shape equation* for the surface. Note that in varying the surface also the surface element dA and the volume element dV change in (4.1).

4.1 Surfaces

Ou-Yang et al use "*vector forms, tensor forms, semi-tensor forms and component forms ... at will*" ([Ou-Yang et al, 99] page 71). This should not be a big surprise: biomembranes are two dimensional surfaces embedded in a three dimensional Euclidean space so *geometrically we know what is going on* and can use other quantities than tensors.

Any point $\mathbf{r}$ on the surface is represented through two independent parameters u_1 and u_2: $\mathbf{r} = \mathbf{r}(u_1, u_2)$. The metric on the surface is then

$$ds^2 = g_{pq} du_p du_q \,, \quad g_{pq} = \frac{\partial \mathbf{r}}{\partial u_p} \cdot \frac{\partial \mathbf{r}}{\partial u_q} \,, \quad p, q = 1, 2 \,.$$

In the expression for ds^2 *the summation convention* (summation over repeated indices) is used; this convention will also be used below. The contravariant tensor g^{pq} is defined by

$$g^{pq} g_{rq} = \delta^p_r \,,$$

where δ^p_r is the Kronecker delta: $\delta^p_r = 1$ for $p = r$ and $\delta^p_r = 0$ for $p \neq r$ (as a matrix g^{pq} is the inverse of g_{pq}). The determinant of g_{pq} is denoted g.

The unit normal $\mathbf{n}$ of the surface at $\mathbf{r}(u_1, u_2)$ is defined by

$$\mathbf{n} = \frac{\frac{\partial \mathbf{r}}{\partial u_1} \times \frac{\partial \mathbf{r}}{\partial u_2}}{\sqrt{g}} = \frac{\mathbf{r}_1 \times \mathbf{r}_2}{\sqrt{g}} \,,$$

where the notation $\mathbf{r}_p(u_1, u_2) = \frac{\partial \mathbf{r}}{\partial u_p}(u_1, u_2)$, $p = 1, 2$, is introduced. If we consider (page 39 in [Ou-Yang et al, 99]) two infinitesimal separated points $\mathbf{r}(u_1, u_2)$ and $\mathbf{r}(u_1 + du_1, u_2 + du_2)$ we can find the infinitesimal vector $d\mathbf{r}$ from $\mathbf{r}(u_1, u_2)$ to $\mathbf{r}(u_1 + du_1, u_2 + du_2)$ through a Taylor-expansion of the vector function $\mathbf{r} = \mathbf{r}(u_1, u_2)$:

$$d\mathbf{r} = \mathbf{r}_1 du_1 + \mathbf{r}_2 du_2 + \frac{1}{2}(\mathbf{r}_{11} du_1^2 + 2\mathbf{r}_{12} du_1 du_2 + \mathbf{r}_{22} du_2^2) + \ldots\ldots\ldots$$

where the notation $\mathbf{r}_{pq}(u_1, u_2) = \frac{\partial^2 \mathbf{r}}{\partial u_q \partial u_p}(u_1, u_2)$, $p, q = 1, 2$, is used (note $\mathbf{r}_{12} = \mathbf{r}_{21}$ for "reasonable" functions). Since $\mathbf{r}_1$ and $\mathbf{r}_2$ span the tangent plane at $\mathbf{r}(u_1, u_2)$ we see that a measure to the second order of the "curved strength" of the surface at $\mathbf{r}(u_1, u_2)$ is

$$\mathbf{n} \cdot d\mathbf{r} = \frac{1}{2}(\mathbf{n} \cdot \mathbf{r}_{11} du_1^2 + 2\mathbf{n} \cdot \mathbf{r}_{12} du_1 du_2 + \mathbf{n} \cdot \mathbf{r}_{22} du_2^2) = \frac{1}{2} L_{pq} du_p du_q$$

with $L_{pq} = \mathbf{n} \cdot \mathbf{r}_{pq}$, $p, q = 1, 2$. L_{pq} is a tensor. The determinant of L_{pq} is denoted L.

The mean curvature H can be calculated as

$$H = \frac{1}{2} g^{pq} L_{pq}$$

and the Gaussian curvature can be calculated as

$$K = \frac{L}{g} \,.$$

With more ingredients of the above type and considering the variation $\mathbf{r}' = \mathbf{r} + \psi \mathbf{n}$ of $\mathbf{r}$ for a small function $\psi(u_1, u_2)$ Ou-Yang et al derive the ***general shape equation*** for vesicles:

$$(p_{out} - p_{in}) - 2\lambda H + k_c(2H + c_o)(2H^2 - c_o H - 2K) + 2k_c \nabla^2 H = 0 \qquad (4.2)$$

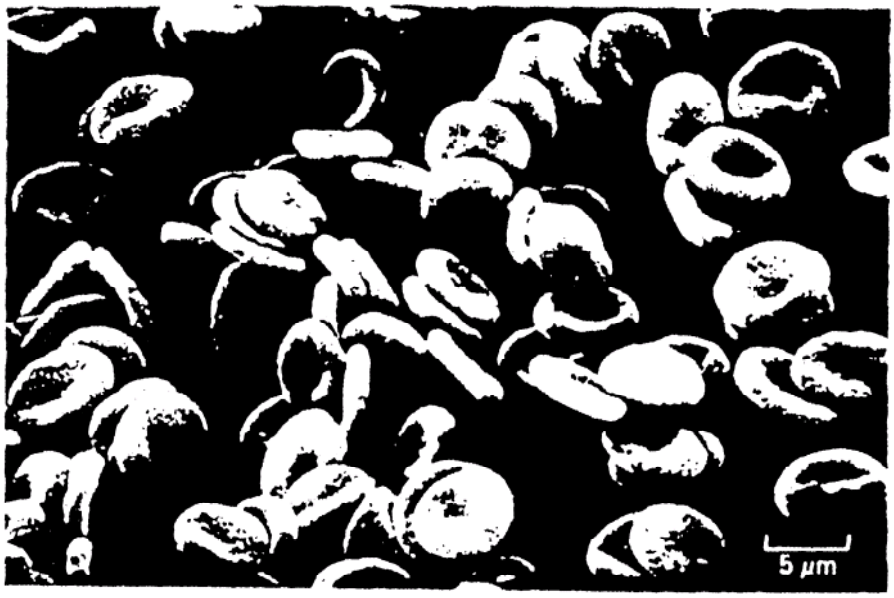

Figure 4.1: [Ou-Yang et al, 99] page 31. Human red blood cells at rest.

for *constant* spontaneous curvature c_o. ∇^2 is the Laplacian operator:

$$\nabla^2\Phi = \frac{1}{\sqrt{g}}\frac{\partial}{\partial u_p}(\sqrt{g}g^{pq}\frac{\partial\Phi}{\partial u_q}) .$$

$\nabla^2\Phi$ is a differential invariant. The general shape equation is the first variation of the expression for the shape energy. Ou-Yang et al derive equations for the second and third variation of the shape energy too; these equations are of use in stability considerations. Ou-Yang et al discuss stability for two exact solutions: spheres and circular cylinders. The general shape equation (4.2) is a complicated *nonlinear* partial differential equation (with fourth order derivatives of $\mathbf{r}$) for which no general analysis have been made yet. Particular solutions exist and below we consider the circular biconcave discoid.

4.2 Circular Biconcave Discoid

Through observations it is known that mature red blood cells of human beings always are in the shape of a biconcave discoid. There is no general classical mathematical theory for biconcave discoidal surfaces, but an expression has been suggested which gives a solution to the general shape equation (4.2).

Due to a reasonable high degree of symmetry of the red blood cells an axisymmetric shape is a good representation. We can let the z-axis be the axis of rotational symmetry. Letting ρ be the distance from the z-axis and θ the angle of rotation in the (x, y)-plane we

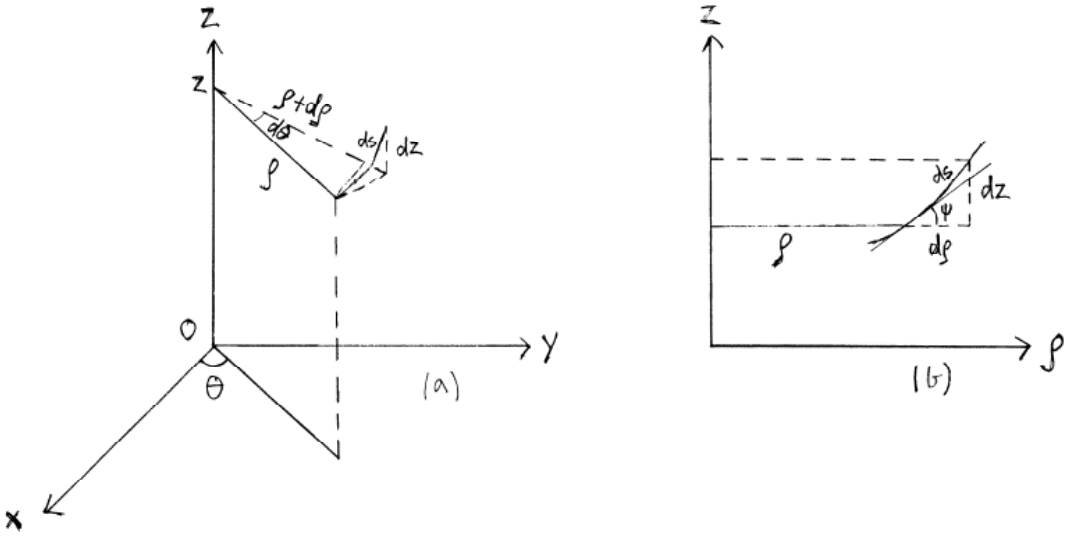

Figure 4.2: Coordinates for description of axisymmetric shapes

have:

$$x = \rho\cos\theta\,, \quad y = \rho\sin\theta\,.$$

With the two independent parameters ρ and θ we consider surfaces $\mathbf{r} = \mathbf{r}(\rho,\theta)$ or explicitly

$$\mathbf{r} = \begin{pmatrix} x(\rho,\theta) \\ y(\rho,\theta) \\ z(\rho,\theta) \end{pmatrix} = \begin{pmatrix} \rho\cos\theta \\ \rho\sin\theta \\ z(\rho,\theta) \end{pmatrix}\,.$$

Axisymmetric surfaces, which we consider, have $z = z(\rho)$. The angle $\psi = \psi(\rho)$, ψ is a dependent parameter, is introduced as the angle between the radial ρ-axis and the tangent line of the contour, that is $\frac{dz}{d\rho} = \tan\psi$, $\psi \in]-\frac{\pi}{2}, \frac{\pi}{2}[$.

We do calculations of the differential geometric quantities presented above:

$$\mathbf{r}_\rho = \frac{\partial\mathbf{r}}{\partial\rho} = \begin{pmatrix} \cos\theta \\ \sin\theta \\ \tan\psi \end{pmatrix}, \quad \mathbf{r}_\theta = \frac{\partial\mathbf{r}}{\partial\theta} = \begin{pmatrix} -\rho\sin\theta \\ \rho\cos\theta \\ 0 \end{pmatrix}$$

$$\mathbf{r}_{\rho\rho} = \begin{pmatrix} 0 \\ 0 \\ \sec^2\psi\frac{d\psi}{d\rho} \end{pmatrix}, \quad \mathbf{r}_{\theta\rho} = \mathbf{r}_{\rho\theta} = \begin{pmatrix} -\sin\theta \\ \cos\theta \\ 0 \end{pmatrix}, \quad \mathbf{r}_{\theta\theta} = \begin{pmatrix} -\rho\cos\theta \\ -\rho\sin\theta \\ 0 \end{pmatrix}$$

$$g_{\rho\rho} = \mathbf{r}_\rho\cdot\mathbf{r}_\rho = 1+\tan^2\psi = \frac{1}{\cos^2\psi} = \sec^2\psi, \quad g_{\theta\theta} = \mathbf{r}_\theta\cdot\mathbf{r}_\theta = \rho^2, \quad g_{\rho\theta} = g_{\theta\rho} = 0, \quad g = \rho^2\sec^2\psi$$

$$\mathbf{n} = \frac{\mathbf{r}_\rho\times\mathbf{r}_\theta}{\sqrt{g}} = \begin{pmatrix} -\sin\psi\cos\theta \\ -\sin\psi\sin\theta \\ \cos\psi \end{pmatrix}$$

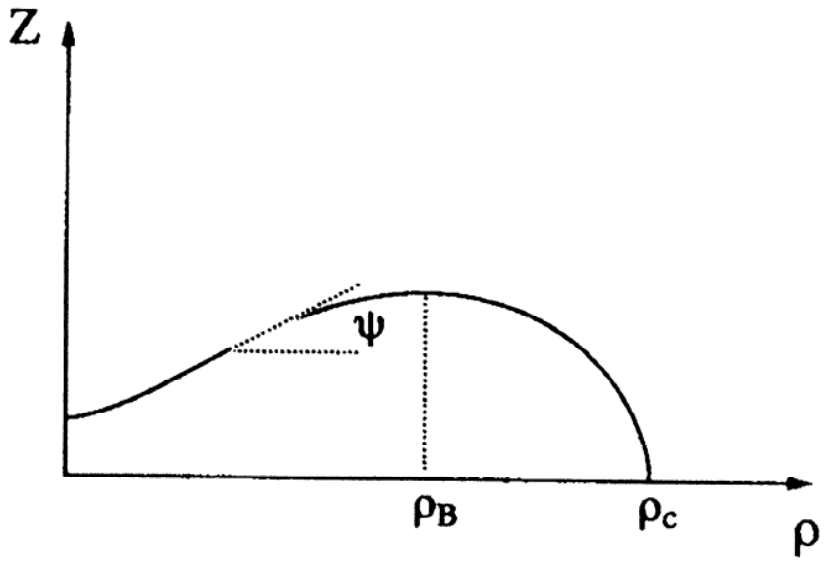

Figure 4.3: [Ou-Yang et al, 99] page 113. Suggested contour.

$$L_{\rho\rho} = \mathbf{n}\cdot\mathbf{r}_{\rho\rho} = \sec\psi\frac{d\psi}{d\rho}, \quad L_{\rho\theta} = L_{\theta\rho} = \mathbf{n}\cdot\mathbf{r}_{\rho\theta} = 0, \quad L_{\theta\theta} = \mathbf{n}\cdot\mathbf{r}_{\theta\theta} = \rho\sin\psi, \quad L = \rho\tan\psi\frac{d\psi}{d\rho}$$

$$H = \frac{1}{2}g^{pq}L_{pq} = \frac{1}{2}(\cos^2\psi\cdot\sec\psi\frac{d\psi}{d\rho} + \frac{1}{\rho^2}\cdot\rho\sin\psi) = \frac{1}{2}(\cos\psi\frac{d\psi}{d\rho} + \frac{1}{\rho}\sin\psi)$$

$$K = \frac{L}{g} = \frac{\sin\psi\cos\psi}{\rho}\frac{d\psi}{d\rho}$$

$$\nabla^2 = \frac{1}{\sqrt{g}}\frac{\partial}{\partial u_p}(\sqrt{g}g^{pq}\frac{\partial}{\partial u_q}) = \frac{\cos\psi}{\rho}\left(\frac{\partial}{\partial\rho}(\rho\cos\psi\frac{\partial}{\partial\rho}) + \frac{\partial}{\partial\theta}(\frac{1}{\rho}\sec\psi\frac{\partial}{\partial\theta})\right).$$

Notice that the mean curvature H and the Gauss curvature K are independent of θ; this reflects the chosen rotational symmetry.

With the above expressions one can calculate the shape equation (a rather lengthly expression) for an axisymmetric surface in the chosen coordinates ([Ou-Yang et al, 99] page 111). A contour, $z = z(\rho)$, suggested for a biconcave discoid is given as:

$$z(\rho) = \int_0^\rho \tan\psi(t)dt, \quad \psi(\rho) = \arcsin\left(\rho(a\ln\rho + b)\right), \tag{4.3}$$

where a and b are constants. Insertion in the general shape equation shows that the surface given by this contour is a rigorous solution provided

$$a = -c_o, \quad p_{out} - p_{in} = 0, \quad \lambda = 0\,.$$

4.3 The Surface Evolver

The above way of handling the problems is more or less the modus vivendi in our reference [Ou-Yang et al, 99]. Another common way of studying the general shape equation is of course to do numerical calculations. A feasible way to do these calculations is using *The Surface Evolver* package [Brakke, 92]. The Surface Evolver package can be found on the world wide web [Evolver, 99].

Chapter 5

Docking Programs

For convenience of the reader, to get some idea of the field, and because the different methods applied in docking programs are of general interest we include some cursory information on docking programs.

The primary reference on docking programs in this thesis [Halperin et al, 02] does not give a summary of the progress of docking programs in the last decade (there should be some references though: see page 409), but is more intended as a view on what has been made and directions for further development.

To what extent the pharmaceutical industry have and make use of docking programs is not evident but the general assumption is that large companies do, [Halperin et al, 02] page 409: "*docking has been heavily used in industry in rational drug design*". An older broad-based reference from a pharmaceutical point of view is Irwin D. Kuntz's [Kuntz, 92] Science-paper: *Structure-Based Strategies for Drug Design and Discovery.*

5.1 Kuntz and Co-workers' DOCK Program

Searching the world wide web for "docking" gave beside what we here investigate a lot of different Internet sites for harbours and also sites for spacecrafts. One entry among six entries in an English dictionary explains "dock" as "*to haul or guide into a dock or to join (e g spacecraft) together while in space*". The use of the term "docking" in connection with biomolecules has to be understood in analogy with this explanation: one biomolecule has to be joined with another biomolecule; the reader is encouraged to look at the Appendix with illustrations from Hex.

Kuntz and co-workers use DOCK [Kuntz, 92] as the name of their computer program (with a reference dating back to 1982) "*that is used to solve the 3-D jigsaw of fitting putative "ligands" into appropriate sites of the receptor".*

5.1.1 Spheres

In DOCK the basic geometrical building blocks modeling the molecules are spheres:

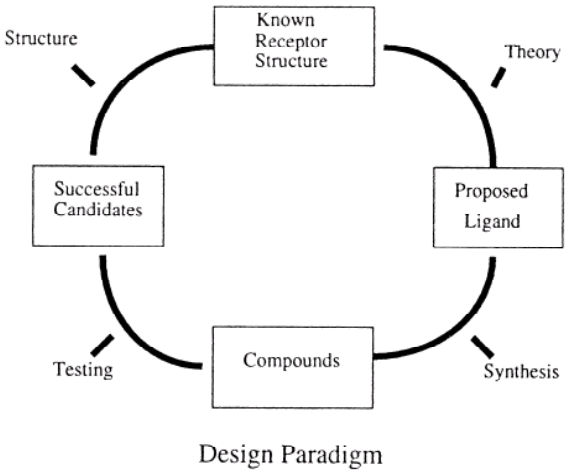

Fig. 1. General approach to the structure-based design of biological inhibitors. Begin with the determination of the structure of the target receptor. Theoretical principles and experimental data are used to propose a series of putative ligands. These compounds are synthesized and tested. The final step is the determination of the structure of the receptor-ligand complex. The figure emphasizes the cyclic and multidisciplinary aspects of this type of project.

Figure 5.1: [Kuntz, 92] page 1079.

"*As a first step, DOCK characterizes the entire surface of the macromolecule, seeking the grooves and invaginations in the surface that form the target sites. These sites are filled with sets of overlapping spheres. A set of sphere centers serves as the negative image of a specific site (Fig. 2). Typically, the sites found by the program include the active regions of enzymes, recognition and allosteric features, and other small pockets that have no known function (45). The program is not restricted to examining enzymes.*"

The process can be reversed:

"*We can also use a "positive image" of a macromolecular surface by reversing the mathematical procedure and producing spheres inside the "receptor" (51).*"

5.1.2 Matching Algorithms and Scoring Functions

Different methods are used to find close fits:

"*The second step in the DOCK algorithm matches x-ray or computer-derived structures of putative ligands (52) to the image of the receptor on the basis of a comparison of internal distances. Matching algorithms come from a well-studied area in combinatorial mathematics called the "isomorphic subgraph" problem (53). Although a systematic search of all ways to fit two objects together is not feasible, rapid heuristic approximations are available (45, 46, 51) that examine thousands of alternative geometric matches per second. Each of these orientations must be evaluated to measure the goodness of fit of the "ligand" to the site.*

> *At first, we used a simple proximity scoring method (12, 45, 54) as a measure of steric complementarity. Recently, we have expanded the scoring functions to include a full intermolecular force field (47).*"

We see that DOCK does not use a systematic search but different methods to find close fits. The program Hex [Ritchie & Kemp, 00] considered later in this thesis exploits a systematic search. As mentioned earlier an example of an intermolecular force field is CHARMM.

5.1.3 Databases

DOCK can be used for evaluating different ligands in databases:

> "*The program searches 3-D databases of small molecules and ranks each candidate on the basis of the best orientations that can be found for a particular molecular conformation (12, 46, 47). Each molecule can be evaluated either on its own merits or as a template. The template concept encourages chemist to look beyond the literal database entries to the design of new chemical species. The ability of DOCK to propose specific molecules in specific orientations in the active site is one of its strongest features. Although some of these molecules are related to substrates, cofactors, or known inhibitors, others can be of novel structures (12).*
>
> *Computer programs such as DOCK can provide a rapid and controlled exploration of the geometric intricaties of target sites. Ligands can be examined at a rate of 10 to 100 per minute, making it possible to examine databases of 100,000 compounds in less than a week with a workstation. Implementing the program on a supercomputer or parallel-processing device makes it possible to search a corporate database of 500,000 compounds in a day.*"

Note, docking algorithms for drug design are somewhat different from protein-protein docking. Especially small molecules (compounds of pharmacophores) are used for drugs ([Halperin et al, 02] page 419).

5.1.4 Discrimination Between Leads

DOCK provides a ranking of the ligands in the searched database. This gives the possibility to look at the leads with a good result:

> "*Typically, the 100 to 200 best-scoring compounds are examined with computer graphics (Table 3).*"
>
> "*In every case we have tried, DOCK has proven extremely valuable as a computer screening procedure and as a method of generating structural hypotheses about ligand-receptor interactions.*"

But this is also somehow the limit of DOCK due to the used approximations:

> "*The use of DOCK to optimize leads has been more problematic. The two major difficulties are obtaining the proper ligand conformation and discriminating among several proposed interaction modes of similar energy (47, 51). Many assumptions are required to scan large databases in a reasonable amount of time. These include: rigid ligands and rigid receptors, neglect of bound water molecules and counterions, and simplified evaluations of interaction energies.*"

And the conclusion in 1992 was:

> "*In sum, DOCK works well as a computer screening procedure for generating leads.*"

5.2 The Review Article of Halperin et al

In the invited review article of Halperin et al [Halperin et al, 02] they consider small (drug) and large protein-protein molecule docking and the problem of going from *rigid* to *flexible* docking. The literature presents the field in non-uniform formats and a goal of the article is to rectify this.

The article is organized through the following headlines:

- Representation of the system,
- Overview of search procedures and matching algorithms,
- Approaches to scoring schemes.

We will shortly discuss these issues.

5.2.1 Representation of the System

The basic input to a docking program are the three-dimensional structures of the receptor and the "ligands": atomic (x, y, z)-coordinates. These structures can be computer-derived or can be found through X-ray and NMR-investigations.

From the atomic coordinates the classical energy can be calculated by means of *empirical potential energy-functions*. More common is to generate *surfaces*. Every atom has a van der Waals radius and it is possible to generate a *van der Waals surface*. Rolling a sphere with the radius of a water molecule on the van der Waals surface creates a more smooth *solvent-accessible molecular surface*. An important program calculating solvent-accessible molecular surfaces was developed by Michael L. Connolly [Connolly, 96] (to visualize a procedure: let water spheres "rain" from all directions onto the van der Waals surface).

We learned above that DOCK used spheres to represent the important geometric features of the surface of the macromolecule. Another type of representation is to use slices of the surface. Physical and chemical features such as polar and nonpolar portions of the

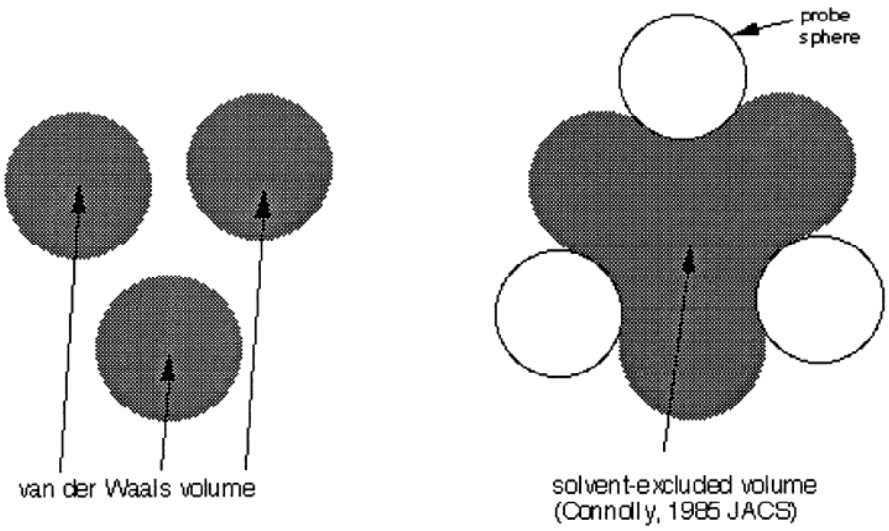

Figure 5.2: [Connolly, 96]. Molecular surface generation.

protein surface can be added to the geometrical description. Different methods can be applied to include flexibility. In rigid body docking "*flexibility is handled through a "soft" belt into which atoms from the second molecule can penetrate*" ([Halperin et al, 02] page 415).

5.2.2 Overview of Search Procedures and Matching Algorithms

Two different kinds of search procedures are used:

- Full solution space search,
- Gradual guided progression through solution space.

Docking is computationally very difficult due to the high amount of rotational and translational orientations of the two molecules. If databases are to be screened and flexibility also is considered the problem becomes even more complicated.

Employing potential energy-functions the criterion for matching is of course to find minima of the energy; the search procedures are often based on statistical, algorithmic or molecular dynamics methods. The Geometric Hashing method, which is based on maxima and minima combined with normals in the shape function for the surfaces, utilizes an algorithm from object recognition in computer vision. The molecular overlap and penetration can be used in Fourier correlation techniques. It is important to emphasize that docking algorithms for protein-protein association differ somewhat from those for small ligand docking used in drug design ([Halperin et al, 02] page 419).

5.2.3 Approaches to Scoring Schemes

In the potential energy-function approach the score for a fit depends on the value of the (classical) energy, in the surface approach the root-mean-squared (RMS) value of the distance between the two surfaces could be a measure for the fit, and for the Fourier correlation techniques, roughly stated, the overlap of thin surface layers has to be maximized and the penetration minimized. Other physical and chemical parameters are of course important for the fit (especially for the non-energetic approaches). Halperin et al discuss the following:

- Geometric complementarity,
- Intermolecular overlap,
- Intra-molecular overlap,
- Hydrogen bonds,
- Contact area,
- Pairwise amino acid and atom-atom contacts,
- Electrostatic interactions and solvation energy in quick scan.

Combined use of different parameters is called *consensus scoring*.

5.3 Other Docking Programs

Different docking-programs exist, above we considered the DOCK-program of Kuntz and his group, below a few other programs or methods are shortly presented. Later we will in detail concentrate on David W. Ritchie's Hex-program [Ritchie & Kemp, 00]. The Cancer Research in the UK has a site on the Internet with links to some docking programs [smithgr, 02].

5.3.1 A Fourier Correlation Technique

In [Katchalski-Katzir et al, 92] they represent the surface of a molecule through a thin surface layer and use the fast Fourier transform algorithm.

The two molecules **a** and **b** are projected onto a three dimensional grid of $N \times N \times N$ points, where they are represented by the discrete functions

$$a_{l,m,n} = \begin{cases} 1 & \textit{inside the molecule} \\ 0 & \textit{outside the molecule}, \end{cases}$$

and

$$b_{l,m,n} = \begin{cases} 1 & \textit{inside the molecule} \\ 0 & \textit{outside the molecule}, \end{cases}$$

where $l, m, n \in \{1, ..., N\}$. Any grid point is considered inside the molecule if there is an atomic nucleus within a distance of the order of magnitude of atomic van der Waals radii from the grid point. To distinguish between the thin surface layer and the interior of the molecule the value of 1 is retained for the surface layer and another value is specified for the interior

$$\overline{a}_{l,m,n} = \begin{cases} 1 & on\ the\ surface\ of\ the\ molecule \\ \rho & inside\ the\ molecule \\ 0 & outside\ the\ molecule, \end{cases}$$

and

$$\overline{b}_{l,m,n} = \begin{cases} 1 & on\ the\ surface\ of\ the\ molecule \\ \delta & inside\ the\ molecule \\ 0 & outside\ the\ molecule. \end{cases}$$

The parameter ρ is assigned large negative values and the parameter δ is assigned small nonnegative values. The *correlation* is defined as

$$\overline{c}_{\alpha,\beta,\gamma} = \sum_{l=1}^{N} \sum_{m=1}^{N} \sum_{n=1}^{N} \overline{a}_{l,m,n} \cdot \overline{b}_{l+\alpha,m+\beta,n+\gamma}, \tag{5.1}$$

where α, β and γ are the number of grid steps by which molecule **b** is translated with respect to molecule **a** in each dimension (note the resemblance with a *convolution*). This correlation function is a measure of the fit between the two molecules. Due to the choice of values for ρ and δ large negative values of the correlation $\overline{c}_{\alpha,\beta,\gamma}$ corresponds to forbidden penetration of the molecules whereas large positive values of $\overline{c}_{\alpha,\beta,\gamma}$ correspond to overlapping of the thin surface layers and a good fit. The values of α, β and γ maximizing $\overline{c}_{\alpha,\beta,\gamma}$ must be found.

The discrete Fourier transform of a function $x_{l,m,n}$ is defined as

$$X_{o,p,q} = \sum_{l=1}^{N} \sum_{m=1}^{N} \sum_{n=1}^{N} \exp[-2\pi i(ol + pm + qn)/N] \cdot x_{l,m,n},$$

where $o, p, q \in \{1, ..., N\}$ and $i = \sqrt{-1}$. The application of this transform to the defining equation (5.1) of the correlation function gives the following result

$$C_{o,p,q} = A^*_{o,p,q} \cdot B_{o,p,q}$$

where C and B are the discrete Fourier transform of the functions $\overline{c}$ and $\overline{b}$ respectively and A^* is the complex conjugate of the discrete Fourier transform of $\overline{a}$. The inverse discrete Fourier transform of $C_{o,p,q}$ is defined as

$$\overline{c}_{\alpha,\beta,\gamma} = \frac{1}{N^3} \sum_{o=1}^{N} \sum_{p=1}^{N} \sum_{q=1}^{N} \exp[2\pi i(o\alpha + p\beta + q\gamma)/N] \cdot C_{o,p,q}.$$

Due to *the fast Fourier transform algorithm* the use of the Fourier transform and the inverse Fourier transform to calculate the correlation $\overline{c}_{\alpha,\beta,\gamma}$ for different values of α, β and γ "*significantly*" reduces the number of steps compared to the number of steps needed in a direct evaluation of (5.1) for different α, β and γ.

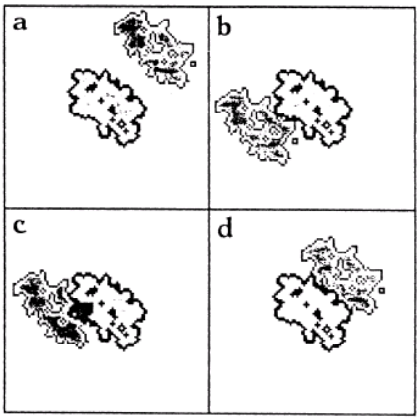

FIG. 2. Different relative positions of molecules a and b, illustrated by the cross sections $\bar{a}_{46,m,n}$ and $\bar{b}_{46,m,n}$ from Fig. 1. The relative orientation of the molecules is as in the known α–β dimer. (*a*) No contact. (*b*) Limited contact. (*c*) Penetration. The penetrated area is represented in black. (*d*) Good geometric match, as indicated by the extensive overlap of complementary surface layers.

Figure 5.3: [Katchalski-Katzir et al, 92] page 2196. Alpha-beta hemoglobin dimer.

5.3.2 The Geometric Hashing Method

The Geometric Hashing method combines the geometrical concept of critical points together with their normals and an algorithm (using a "*hash table data structure*") from object recognition in computer vision ([Norel et al, A, 94], [Norel et al, B, 94], [Fisher et al, 95]; corresponding author on these three articles was Ruth Nussinov).

The critical points correspond to "*knobs*" (convex regions) and "*holes*" (concave regions) in the surface. Based on Connolly's Molecular Surface algorithm a shape function measuring the convexity or concavity of the surface can be defined and the critical points can be determined.

Very important also a *normal* can be calculated at the critical points ([Norel et al, A, 94] page 935):

> "*To determine a transformation that superposes one body onto another, one needs a minimum of three (noncollinear) matching point pairs in both objects. However, three or four matching knob-hole point pairs are not always present at the receptor-ligand interface. Indeed, that might have been the reason why Connolly failed in his matching scheme to correctly dock the trypsin inhibitor into its trypsin receptor.*[3,4]
>
> *A critical difference between our approach and previous ones is the employment of the surface normals. This enables using only two critical points in the calculation of the transformation. The normal itself serves as the third (and fourth) point. Thus not only are we able to dock receptor-ligand surfaces*

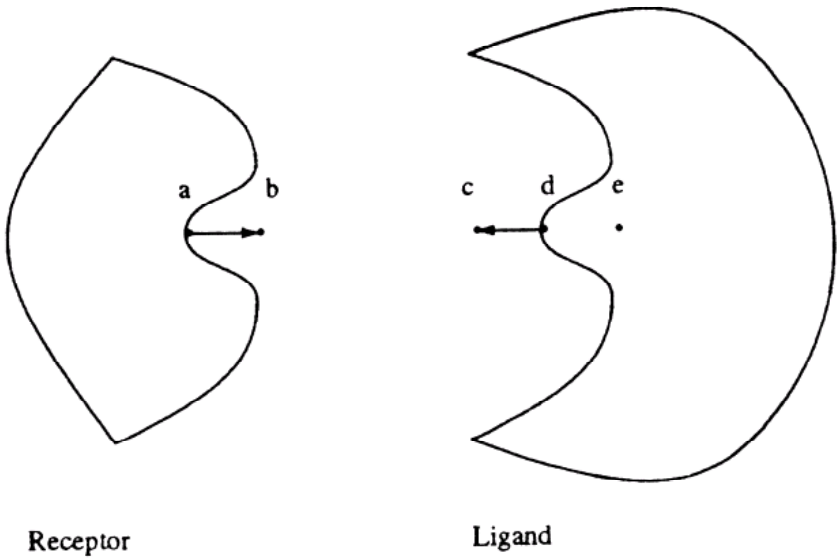

Figure 1. Critical points and their normals.

Figure 5.4: [Norel et al, A, 94] page 936.

with only two knobs/holes point matches combination, but the complexity of the docking method is reduced as well."

To some extent (for instance also a concept of *signatures* is introduced) the procedure for matching is described the following way ([Norel et al, A, 94] page 936):

"*For each pair of critical points from one molecule (e.g., the receptor), we compute the transformation with each compatible pair from the second molecule (e.g., the ligand). Compatibility implies that a knob must be paired with a hole (and vice versa). In the second molecule (the ligand) the "normals" are inverted. The points that are one unit away from the critical points, in the normal orientation, are aligned as well. For example, in Figure 1 point "a" is aligned with point "d," and point "b" is aligned with point "e," which is reversed from c.*

For a first reading on details of the used matching-algorithm [Fisher et al, 95] is recommended. A short description of "*The hash table data structure*" can be found at page 46 in [Norel et al, B, 94].

The discrimination between leads is still a problem ([Norel et al, A, 94] page 939):

"*Being too restrictive at the matching stage may result in skipping the correct solutions altogether. For this reason, the logic adopted in this work has been*

to include correct solutions along with "false positives" first, filtering the latter later."

The Geometric Hashing method is apparently fast ([Halperin et al, 02] page 418):

"*Unlike the traditional methods, the Geometric Hashing-based matching algorithm is one of the unique fundamental methods used in docking that can deal with such a complexity efficiently. The algorithm was originally suggested for object recognition in computer vision.*[141] *Combined with an adequate molecular surface representation, it yields a state-of-the-art tool-kit for docking.*[36,37,39–44] *Fourier correlation techniques are also widely used. Usually, three-dimensional grid-based fast-Fourier transform (FFT) docking correlation methods are slow; however, more efficient searching may be obtained using spherical polar Fourier correlations.*[46] *Consider, for example, the so-called rigid-body docking (which, despite its name, still allows surface variability). Currently, there is a vast variability in the search performance of the available algorithms. Some matching programs, such as those represented by the FFT,*[142] *take on the order of days of CPU.*[78,143–148] *This is owing to the exhaustive conformational space search procedure inherent to the FFT procedure. Others, such as the Geometric Hashing,*[39–44] *focus only on the relevant conformational space, and reach similar results in minutes.*"

It should be noted that two authors (Ruth Nussinov and Haim Wolfson) of the review [Halperin et al, 02] also are authors of the Geometric Hashing method articles:
[Norel et al, A, 94], [Norel et al, B, 94] and [Fisher et al, 95]. In [Ritchie & Kemp, 00] page 178 the following comment is made on the quick geometric methods as compared to FFT-methods concerning the problem of discrimination between leads or "real" and "false positives":

"*However, such geometric methods generally require a post-processing step to remove sterically prohibited orientations.*[16,21] *In contrast, the Fourier correlation approach*[22] *uses a simple Cartesian grid model of protein topology which favors close contacts and automatically penalizes steric clashes."*

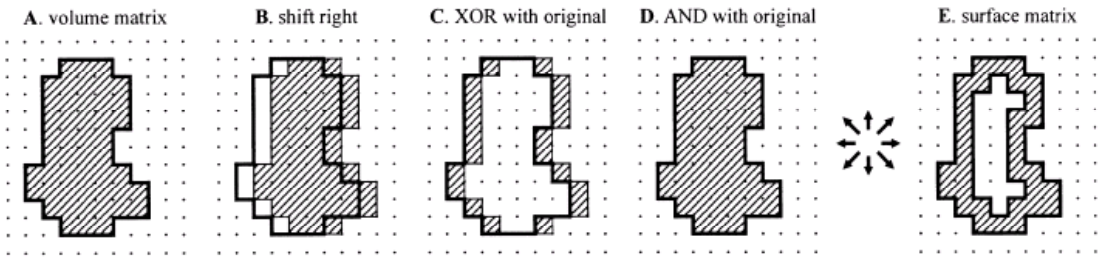

Fig. 2. Schematic representation (two-dimensional) of the surface determination process. **A:** The volume matrix occupied by the protein is outlined with a thick black line. **B:** A copy of the matrix (gray) is shifted one location relative to the original (*heavy contour*). **C:** XOR operation *between both matrices* eliminates (turns to *0*) all *overlapping* locations. Two partial shells are left (*gray cells*), one belonging to the original and the other belonging to the copy (outside the original contour). **D:** The outer shell fragment is eliminated by an AND operation with the original *matrix* (heavy contour). **E:** The previous steps are repeated in all directions (*including diagonals*) and the partial surface shells are *finally* added with OR operations. The resulting surface shell is composed solely of surface locations belonging to the original shape (gray).

Figure 5.5: [Palma et al, 00] page 376.

5.3.3 A Digital Grid-Based Program: BiGGER

Another interesting docking program is BiGGER: Bimolecular Complex Generation with Global Evaluating and Ranking [Palma et al, 00]. The molecules are digitally (zero/false or one/true) represented in a three-dimensional real space grid with 1Å side-lengths. No Fourier-transform is employed but a shrewd use of Boolean AND, XOR and OR-operations makes docking of two molecules possible in "*2 to 8 hours of CPU time*" "*on widely available personal computers*". As one among other important features the algorithm allows flexibility of amino acid side chains.

BiGGER uses geometric complementarity and amino acid pairwise affinities in a first search step. A scoring function in a second search step is based on "*geometric complementarity of the surfaces, explicit electrostatic interactions, desolvation energy, and pairwise propensities of the amino acid side chains to contact across the molecular surface*". A neural network using a learning set of 25 known protein-protein complexes has been applied to optimize the scoring function.

The BiGGER docking algorithm is a "soft" algorithm. The notion of "softness" in docking algorithms is not precise; maybe as a general idea "softness" is to avoid throwing away possible docking solutions or everything that make the rigid-body approximation "less rigid". In BiGGER this is implemeted in different ways, for example allowing a coarse molecular surface due to the digitization. "Softness" is important due to the conformational changes that can happen in real protein-protein associations. According to these changes one distinguishs between *bound*, *unbound* and *pseudo-unbound* docking; compared to the explanation in [Halperin et al, 02] (page 410) a more readable explanation of these terms is given in [Palma et al, 00] (page 374):

> "*A collection of 25 protein-protein complexes with experimentally (X-ray and NMR) determined structures was used as learning and test sets (Table I). These were chosen from complexes of different types, including several examples of dimeric proteins, protease-(proteic) inhibitor, antibody-antigen, and complexes*

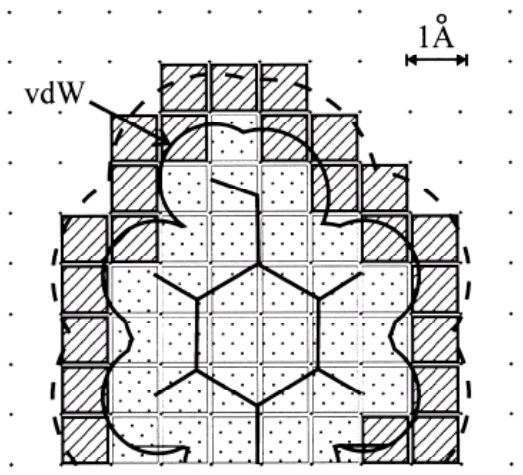

Fig. 1. Schematic representation of a digitized molecular fragment. The side chain of a planar tyrosine residue is represented by its van der Waals surface contour (solid). The molecular shape is placed into a regular Cartesian grid of 1Å unit size and every grid position is assigned to the molecular volume (will have a value of *1*) if its center lies within 1Å (dashed contour) of the van der Waals surface. All other cells represent the exterior of the molecular volume and are assign a value of *0* (False). The outer cubes of this representation (filled with slanted lines) will be subsequently assigned as surface shell and the remaining inner positions will constitute the molecular core (dot-filled cubes).

Figure 5.6: [Palma et al, 00] page 375.

between electron transfer proteins. Furthermore in order to test the ability of the program to handle the conformational changes that occur upon formation of the complexes, two quality tests were performed: in the first 6 cases the complexes were reconstructed from the structures of the co-crystallized proteins, after being taken apart from the complex and randomly orientated. In these cases, the conformations of the two molecules are already "adapted" to each other and this set of docking simulations is designated as bound in Table I. In all other cases, the complexes were predicted using the unbound or native conformations of both interacting proteins (unbound) or at least, of one of the two (pseudo-unbound)."

The goal is to develop docking algorithms that are able to treat the real *unbound* case.

The BiGGER algorithm exploits the "soft belt"-flexibility method shortly discussed above ([Palma et al, 00] page 375):

"*Treating this molecular flexibility in an explicit way would be an impracticable computational task. However, the technique used in this work incorporates side chain flexibility, implicitly, in the definiton of a soft molecular surface. This is based on the observation that most of the conformational changes occuring upon complex formation are due to flexible amino acid side chains positioned at the molecular surface (Fig. 3). Moreover, not every amino acid shows*

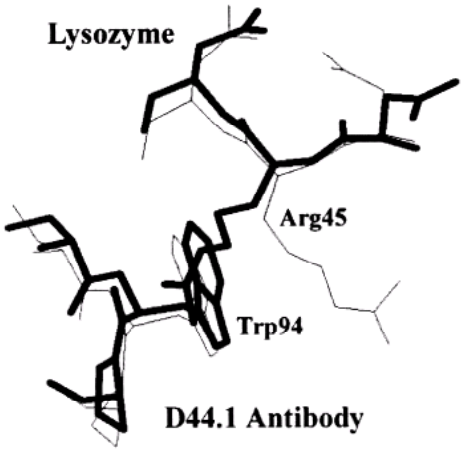

Fig. 3. Detail of the interaction between monoclonal antibody D44.1 Fab fragment (1mlb) and lysozyme (1lza). Thin lines correspond to the X-ray structure of the complex, while thick lines show the conformations of the non-complexed antibody and lysozyme structures, when superposed on that of the crystallographic complex (1mlc). A large conformational difference of Arg45 side chain atoms is revealed, while the relative positions of the main chain atoms are mostly preserved. A major clash between Trp94 of the antibody and Arg45 of lysozyme is expected, if the free structures of the two proteins are docked to each other as rigid bodies.

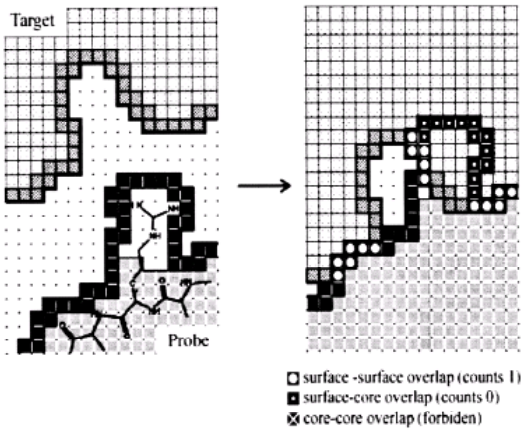

Fig. 4. Schematic representation of the surface matching evaluation. Flexible amino acid side chains are assigned a "soft" shape by eliminating (setting to *0*) every core positions belonging to side chain atoms other than carbon β. This produces a hollow surface shell with the same shape. For every relative position of the two interacting proteins (actually, their digital representations), the extent of their surface matching is evaluated by the number of surface cells of the target molecule overlapping surface cells of the probe. Although allowed to occur, overlaps between surface and core cells do not contribute (they count *0*) for the matching evaluation. Finally, every solution that results in the overlapping of core cells from both molecules is immediately discarded, thus rejecting solutions involving unrealistic interpenetration of the docking partners.

Figure 5.7: [Palma et al, 00] page 376-377. In particular, note the "soft belt" in Fig. 4.

> *the same degree of freedom to move. Amongst the protein complexes observed, ARG, LYS, ASP, GLU, and MET present the highest frequency and amplitude of movements between the structures of free and co-crystalized proteins. So, every atom (except carbon β) belonging to the side chains of these amino acids is considered flexible and is allowed to unrealistically penetrate the other molecule during the docking search.*"

5.3.4 Protein Structure Variations: FLEXE

In [Claußen et al, 01] it is possible to get more information about flexible docking methods. The introduced FLEXE program is based on the previous FLEXX program. FLEXX can deal with flexibility of ligands ([Claußen et al, 01] page 390):

> "*The conformational flexibility of the ligand is modeled by a discrete set of prefered torsion angles at acyclic single bonds, and multiple conformations for ring systems. Torsion angles at multiple bonds, bond lengths and bond angles are used as given in the input structure. The torsion angles are taken from a database containing about 900 molecular fragments with a central single bond which has been derived from the Cambridge Structure Database (CSD)*[42] *by Klebe & Mietzner.*[43] *By this method up to 12 low-energy torsion angles can be assigned to each single bond.*"

The new concept of FLEXE, an ensemble of protein structures which represents the flexibility, is introduced the following way ([Claußen et al, 01] page 390):

> "*The FLEXE approach is based on the united protein description which handles the similarities and differences of the protein structures of the ensemble. All side-chains and backbone parts are treated seperately and the dependencies between them are represented in the so-called incompatibility graph. An algorithm for finding sets of pairwise compatible instances is applied to this graph to ensure that valid docking structures are used as a basis for the docking algorithm. These steps are described in more detail in the following sections.*"

FLEXE apparently, among other methods, uses graph-theory. "*FLEXE takes about five and a half minutes on average for placing one ligand into the united protein description on a common workstation*" ([Claußen et al, 01] page 377).

5.3.5 Genetic Algorithms and Molecular Mechanics: DARWIN

The program DARWIN is described in [Taylor & Burnett, 00]. DARWIN does not use geometrical matching instead the classical energy is evaluated using the molecular mechanics program CHARMM. Since CHARMM can evaluate energies for different atomic coordinates flexible molecules can be docked. Of course this is very computationally costly and the program does not perform a full solution space search but uses a standard genetic algorithm to "*optimize the molecules's conformation and orientation under the selective pressure of minimizing the potential energy of the complex*" ([Taylor & Burnett, 00] page 173).

It should be noted that DARWIN can take *solvent effects* into account (page 175 and 176 in [Taylor & Burnett, 00]):

> "*Initial experiments showed that docking a target and ligand in a vacuum, i.e., without including water molecules, did not always yield the correct solution. A likely explanation is that without water, the electrostatic portion of the evaluation was inaccurate and so gave misleading results.*"
>
> "*Instead, the system's electrostatic potential energy, which includes the hydrophobic and charged effects of bulk solvent, was modeled with the program "Qnifft" (Dr. Kim Sharp, personal communication).*"
>
> "*The atoms were charged using the same partial charge values as used for the CHARMM calculations. The boundary conditions at the edge of the box were computed using the dipolar option, with a solvent dielectric of 80 and an interior dielectric of 4. Salt effects were calculated for an ionic strength of 0.145 M, using an ion-exclusion radius of 2 Å. The solution to the non-linear Poisson-Boltzmann equation was assumed to have reached convergence when the residual dropped below* 1×10^{-3} *(the default value).*"

As an important computational feature DARWIN utilizes a parallel interface allowing it to be run on several CPUs. DARWIN could not totally solve the common problem of "false positives" ([Taylor & Burnett, 00] page 173 (from the Abstract)):

> "*The method was applied to three protein-carbohydrate complexes: the crystallographically determined structures of Concanavalin A and Fab Se155-4; and a model structure for Fab ME36.1. Conformations close to the crystal structures were obtained with this approach, but some "false positive" solutions were also selected. Many of these could be eliminated by introducing different methods for simulating solvent effects. An effective screening method for docking a database of compounds to a single target enzyme using DARWIN is also presented.*"

As a final remark it must be stressed that although it is impressing that it is possible to use molecular mechanics in a docking-procedure it still is *not a quantum approach.*

Part II

Ritchie's *Hex* program

Chapter 6

Methods

David W. Ritchie and Graham J. L. Kemp [Ritchie & Kemp, 00] use spherical polar Fourier correlations in Ritchie's docking program: *Hex*. It is worthwhile to consider Hex in detail. Hex is a program for large protein-protein docking.

With the review article of Halperin et al [Halperin et al, 02] in mind we try to organize our first look at the methods of Hex according to the following headlines:

- Representation of the system,
- Overview of search procedures and matching algorithms,
- Approaches to scoring schemes.

6.1 Shape Complementarity and Electrostatics

Hex uses the rigid-body approximation, that is, the molecules are considered to be non-flexible. The first task of Hex is to exploit shape complementarity of the protein surfaces. The second task of Hex is to exploit classical electrostatics.

6.1.1 The "Double Skin" Model

With protein input as a pdb-file (pdb: protein data base) of the atomic (x, y, z)-coordinates a dot representation of the molecular surface is produced rolling a probe sphere over the van der Waals surface of the molecule. Due to the dot representation integration can be performed as summation. Ritchie and Kemp use their own algorithm. We can not go into details about this here.

Two "skins" are generated connected to a protein surface: an exterior skin and an interior skin. The exterior skin is defined as the volume bounded by the molecular surface and the solvent-accessible surface (which is offset from the molecular surface by the radius of the probe sphere). The interior skin is defined as the union of the van der Waals volumes of all atoms just inside the molecular surface. The skin thickness used in Hex is 1.4Å.

Fig. 2. A cartoon illustration of protein shape complementarity with the "double skin" model. The exterior skin is the volume bounded by the solvent-accessible surface (dashed lines) and the molecular surface (solid lines). Shaded regions represent interior skins. On moving from the orientation in (a) to that of (b) so as to maximize the degree of overlap between respective pairs of interior and exterior skins, an inevitable consequence is to bring the two surfaces into very close contact. The central hatched area shows the solvent-accessible volume occluded on association.

Figure 6.1: [Ritchie & Kemp, 00] page 183.

The skins are represented as characteristic functions; $\sigma(\mathbf{r})$ for the exterior skin and $\tau(\mathbf{r})$ for the interior skin:

$$\sigma(\mathbf{r}) = \begin{cases} 1 & for\ \mathbf{r} \in exterior\ skin, \\ 0 & otherwise, \end{cases}$$

$$\tau(\mathbf{r}) = \begin{cases} 1 & for\ \mathbf{r} \in surface\ atom, \\ 0 & otherwise. \end{cases}$$

The shape complementarity score S for protein A, with exterior skin σ_A and interior skin τ_A, and protein B, with exterior skin σ_B and interior skin τ_B, is now defined as

$$S = \int \sigma_A(\mathbf{r})\tau_B(\mathbf{r})dV + \int \sigma_B(\mathbf{r})\tau_A(\mathbf{r})dV - Q\int \tau_A(\mathbf{r})\tau_B(\mathbf{r})dV\,. \tag{6.1}$$

The first two terms calculate overlaps between the exterior and interior skins which are to be maximized. The third term describes steric forbidden interior-interior skin overlap: Q is a penalty factor. Hex uses $Q = 12$. In this way Hex automatically penalizes steric clashes in contrast to methods based upon "knobs", "holes" and associated normals such as the geometric hashing method ([Ritchie & Kemp, 00] page 178).

6.1.2 Electrostatics

With pdb-files for protein A and protein B as input the charge distribution $\rho(\mathbf{r}) = \rho_A(\mathbf{r}) + \rho_B(\mathbf{r})$ on the molecular or atomic level is essentially known. From the charge distribution the potential $\phi(\mathbf{r}) = \phi_A(\mathbf{r}) + \phi_B(\mathbf{r})$ can be derived and the electrostatic energy E can be calculated

$$E = \frac{1}{2}\int (\rho_A(\mathbf{r}) + \rho_B(\mathbf{r})) \cdot (\phi_A(\mathbf{r}) + \phi_B(\mathbf{r}))dV\,. \tag{6.2}$$

Because the derivation of the potential ϕ from the charge distribution ρ is related to translations and rotations we postpone the investigation of the electrostatic energy E to the next section.

6.2 Translations, Rotations and Expansions

We now try to explain how translations, rotations and expansions are used in Hex using our own exposition.

If $f : R^3 \to R$ is a function on the three-dimensional Euclidean space with support $\overline{\{\mathbf{r} \in R^3 | f(\mathbf{r}) \neq 0\}}$, the corresponding function with support translated in the direction $\mathbf{r}_o \in R^3$ is $\mathcal{T}_{\mathbf{r}_o} f$, where the translation operator $\mathcal{T}_{\mathbf{r}_o}$ is defined through

$$(\mathcal{T}_{\mathbf{r}_o} f)(\mathbf{r}) = f(\mathbf{r} - \mathbf{r}_o).$$

Rotations can be accomplished through orthogonal transformations. A real matrix O is orthogonal if

$$OO^t = I\,,$$

where O^t is the transpose of O and I is the identity matrix. Due to this definition we have

$$1 = \det(I) = \det(OO^t) = \det(O)\det(O^t) = \det(O)^2$$

and therefore

$$\det(O) = \pm 1.$$

The orthogonal $n \times n$-matrices constitute a group, O(n), with matrix-multiplication as composition. The orthogonal $n \times n$-matrices with determinant 1 constitute a subgroup, SO(n). The group SO(3) corresponds to three-dimensional *rotations* without reflections.

The analogue notion for complex matrices is the unitary matrices. A matrix U is unitary if it satisfies $UU^\dagger = I$, where $U^\dagger$ is the complex conjugate and transpose of U. U(n) is the group of unitary $n \times n$-matrices and SU(n) is the subgroup of unitary matrices with determinant 1. SO(3) is a subgroup of SU(2).

If $f : R^3 \to R$ is a function, the corresponding function with support rotated according to $O \in$SO(3) is $\mathcal{R}_o f$, where the rotation operator $\mathcal{R}_o$ is defined the following way:

$$(\mathcal{R}_o f)(\mathbf{r}) = f(O^{-1}\mathbf{r})\,.$$

Here O^{-1} is the inverse matrix of O and $\mathbf{r}$ has to be understood as a 3×1-coordinate vector corresponding to the chosen orthonormal basis of R^3. Notice that the translation operator and the rotation operator *do not commute.*

Suppose we have a function $f : R^3 \to R$ and N functions $\chi_i : R^3 \to R$, $i = 1, ..., N$. We can write

$$f = \sum_{i=1}^{N} c_i \chi_i \, + \, \xi_N\,, \tag{6.3}$$

with $c_i \in R$ and $\xi_N = f - \sum_{i=1}^{N} c_i \chi_i$. Applying the linear operators $\mathcal{T}_{\mathbf{r}_o}$ and $\mathcal{R}_o$ to this expression we find respectively

$$\mathcal{T}_{\mathbf{r}_o} f = \sum_{i=1}^{N} c_i \mathcal{T}_{\mathbf{r}_o} \chi_i \, + \, \mathcal{T}_{\mathbf{r}_o} \xi_N\,,$$

$$\mathcal{R}_o f = \sum_{i=1}^{N} c_i \mathcal{R}_o \chi_i + \mathcal{R}_o \xi_N \, .$$

We now assume that the functions χ_i, $i = 1, ..., N$, transform among themselves under the translation and rotation operators, that is, we have

$$\mathcal{T}_{\mathbf{r}_o} \chi_i = \sum_{j=1}^{N} t_{ij} \chi_j \, , \; i = 1, ..., N, \tag{6.4}$$

and

$$\mathcal{R}_o \chi_i = \sum_{j=1}^{N} r_{ij} \chi_j \, , \; i = 1, ..., N, \tag{6.5}$$

where $t_{ij}, r_{ij} \in R$. We get

$$\mathcal{T}_{\mathbf{r}_o} f = \sum_{i=1}^{N} c_i \left(\sum_{j=1}^{N} t_{ij} \chi_j \right) + \mathcal{T}_{\mathbf{r}_o} \xi_N = \sum_{j=1}^{N} \left(\sum_{i=1}^{N} t_{ij} c_i \right) \chi_j + \mathcal{T}_{\mathbf{r}_o} \xi_N \, ,$$

$$\mathcal{R}_o f = \sum_{i=1}^{N} c_i \left(\sum_{j=1}^{N} r_{ij} \chi_j \right) + \mathcal{R}_o \xi_N = \sum_{j=1}^{N} \left(\sum_{i=1}^{N} r_{ij} c_i \right) \chi_j + \mathcal{R}_o \xi_N \, .$$

Successive application of the operators can be written

$$\mathcal{R}_o \mathcal{T}_{\mathbf{r}_o} f = \sum_{j=1}^{N} \left(\sum_{i=1}^{N} t_{ij} c_i \right) \left(\sum_{k=1}^{N} r_{jk} \chi_k \right) + \mathcal{R}_o \mathcal{T}_{\mathbf{r}_o} \xi_N = \sum_{k=1}^{N} \left(\sum_{j=1}^{N} \sum_{i=1}^{N} r_{jk} t_{ij} c_i \right) \chi_k + \mathcal{R}_o \mathcal{T}_{\mathbf{r}_o} \xi_N \, ,$$

$$\mathcal{T}_{\mathbf{r}_o} \mathcal{R}_o f = \sum_{j=1}^{N} \left(\sum_{i=1}^{N} r_{ij} c_i \right) \left(\sum_{k=1}^{N} t_{jk} \chi_k \right) + \mathcal{T}_{\mathbf{r}_o} \mathcal{R}_o \xi_N = \sum_{k=1}^{N} \left(\sum_{j=1}^{N} \sum_{i=1}^{N} t_{jk} r_{ij} c_i \right) \chi_k + \mathcal{T}_{\mathbf{r}_o} \mathcal{R}_o \xi_N \, .$$

In conclusion we see that successive rotations and translations with the assumptions made above always result in an expression of the following form

$$\mathcal{O}\mathcal{P} f = \sum_{k=1}^{N} \eta_k \chi_k + \zeta_N \, ,$$

where $\mathcal{O}\mathcal{P}$ are the successive operations, $\eta_k \in R$ are the coefficients after successive rotations and translations, and $\zeta_N = \mathcal{O}\mathcal{P}\xi_N = \mathcal{O}\mathcal{P}\left(f - \sum_{i=1}^{N} c_i \chi_i\right)$.

If we further assume that the functions χ_i, $i = 1, ..., N$ are *orthonormal* with respect to the L^2 - inner product: $< f, g >= \int f(\mathbf{r}) \overline{g(\mathbf{r})} dV$, we can calculate integrals of the type appearing in (6.1) and (6.2) after rotations and translations (we only consider real functions):

$$\int (\mathcal{O}\mathcal{P}_A f_A)(\mathbf{r}) (\mathcal{O}\mathcal{P}_B f_B)(\mathbf{r}) dV = \sum_{k=1}^{N} \eta_{Ak} \eta_{Bk} + \tag{6.6}$$

$$\sum_{k=1}^{N} \eta_{Ak} < \chi_k, \zeta_{BN} > + \sum_{k=1}^{N} \eta_{Bk} < \zeta_{AN}, \chi_k > + < \zeta_{AN}, \zeta_{BN} > \, .$$

Of course $\xi_N = f - \sum_{i=1}^{N} c_i \chi_i$ introduced above is the notion of an "error", and we see that the last three terms on the right hand side of (6.6) cancel if $\xi_{AN} = 0$ and $\xi_{BN} = 0$, just leaving the calculation of an usual Euclidean inner product:

$$\xi_{AN} = 0,\ \xi_{BN} = 0: \qquad \int (\mathcal{OP}_A f_A)(\mathbf{r})(\mathcal{OP}_B f_B)(\mathbf{r}) dV = \sum_{k=1}^{N} \eta_{Ak}\eta_{Bk} = \underline{\eta}_A \cdot \underline{\eta}_B \,. \tag{6.7}$$

6.2.1 Search Procedure

The orientations of the two molecules A and B have to be varied until the best shape complementarity score S (6.1) and the smallest electrostatic energy E (6.2) are found. Hex uses a search procedure which in principle is a full solution space search; in practice a uniform but discrete variation of five rotation angles and one translational distance is applied.

In practice Hex calculates S and E for different orientations (translations and rotations) as a sum of inner products as in (6.7) and therefore *neglects the terms corresponding to* ξ_N-functions. It is crucial that the chosen functions give good representations with "small" error-functions. Hex uses *two spherical polar expansions*: one for the surface skins and one for the charge distributions and the potentials. See below how the coefficients in such an expansion easily are calculated provided the functions are orthonormal. We consider the actual expansions later.

Above we considered rotations as seen from one origin. This is not the natural way to accomplish rotations. It is geometrically more obvious to perform rotations in the local coordinate systems of molecule A and molecule B respectively. These coordinate systems could have the center of mass of the molecules as their respective origins; Hex takes the origin of each protein as the center of mass of *all heavy atoms* ([Ritchie & Kemp, 00] page 181). A rotation in a local coordinate system can be performed after a translation to the origin of the common coordinate system and back again so the above analysis is still true.

Due to the three degrees of freedom of a rigid body the search space for the best geometrical fit between two rigid bodies or the smallest electrostatical energy is six-dimensional. In Hex the distance between the local coordinate systems of the two molecules together with five Euler angles are used in the search of the best orientations.

For every search step it is neccessary to calculate coefficients $t_{ij} \in R$ and $r_{ij} \in R$ responsible for translation and rotation transformations respectively. In Hex the r_{ij}-coefficients are calculated by means of an analytical expression; more about this and the t_{ij}-coefficients below.

6.2.2 Electrostatics

A charge distribution $\rho(\mathbf{r})$ and a potential $\phi(\mathbf{r})$ are connected through Poisson's equation:

$$\nabla^2 \phi(\mathbf{r}) = -4\pi\rho(\mathbf{r}) \,, \tag{6.8}$$

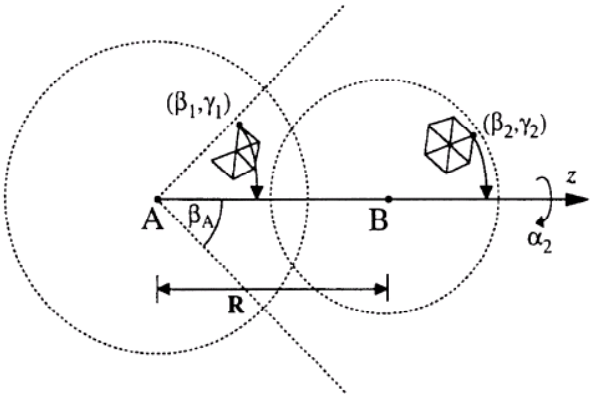

Fig. 3. Schematic illustration of a six-dimensional docking search using tessellated icosahedra. A and B label the receptor and ligand local coordinate origins, respectively. The angular coordinates of each tessellation vertex provide molecular rotational increments (β, γ). If desired, the search may be localized to a known binding site on protein A, assumed to be centered on the z-axis, by calculating the correlation only for orientations where $\beta_1 \leq \beta_A$. A similar constraint may also be applied to β_2 if the ligand epitope is known.

Figure 6.2: [Ritchie & Kemp, 00] page 183.

where ∇^2 is the Laplacian operator. The classical electrostatic energy E is given by

$$E = \frac{1}{2} \int \rho(\mathbf{r})\phi(\mathbf{r})dV. \tag{6.9}$$

On the atomic level each of the proteins A and B have known distributions ρ_A and ρ_B of point charges respectively. The total charge distribution is $\rho(\mathbf{r}) = \rho_A(\mathbf{r}) + \rho_B(\mathbf{r})$ and therefore also known.

If ϕ_A is a solution to Poisson's equation for the charge distribution ρ_A, $\nabla^2\phi_A(\mathbf{r}) = -4\pi\rho_A(\mathbf{r})$, and ϕ_B is a solution for the charge distribution ρ_B, $\nabla^2\phi_B(\mathbf{r}) = -4\pi\rho_B(\mathbf{r})$, then due to the linearity of Poisson´s equation (6.8) the potential ϕ corresponding to the charge distribution $\rho = \rho_A + \rho_B$ can be found as the sum of the solutions ϕ_A and ϕ_B: $\phi = \phi_A + \phi_B$. For the problem at hand vanishing ϕ_A and first derivatives of ϕ_A at infinity would be the obvious, necessary boundary conditions; correspondingly for ϕ_B.

Without comment Ritchie and Kemp find the solution ϕ_A to Poisson's equation for a given charge distribution ρ_A and calculate the electrostatic energy E for different orientations (one could denote it $\mathcal{OP}E$) by means of (6.9) with translated and rotated charge distribution $\mathcal{OP}\rho_A$ and potential $\mathcal{OP}\phi_A$, where as above $\mathcal{OP}$ means some successive translations and rotations; correspondingly for ρ_B and ϕ_B. From a physical point of view this is the obvious way to search for the smallest electrostatic energy but from a mathematical point of view it has to be proved that $\mathcal{OP}\phi_A$ is in fact a solution to Poisson's equation (6.8) with $\mathcal{OP}\rho_A$ as charge distribution. We do this now.

If $\phi(\mathbf{r})$ is a solution to Poisson's equation with charge distribution $\rho(\mathbf{r})$, that is $\nabla^2\phi(\mathbf{r}) = -4\pi\rho(\mathbf{r})$, then $\widetilde{\phi}(\mathbf{r}) = \phi(\mathbf{r} - \mathbf{r}_o)$ will be a solution to Poisson's equation with the charge

distribution $\widetilde{\rho}(\mathbf{r}) = \rho(\mathbf{r} - \mathbf{r}_o)$: $\nabla^2\widetilde{\phi}(\mathbf{r}) = -4\pi\widetilde{\rho}(\mathbf{r})$. Simply use the chain rule twice to see that $\nabla^2\widetilde{\phi}(\mathbf{r}) = \nabla^2\phi\mid_{\mathbf{r}-\mathbf{r}_o}$.

If $O \in$SO(3) then $\widehat{\phi}(\mathbf{r}) = \phi(O^{-1}\mathbf{r})$ also will be a solution to Poisson's equation with the charge distribution $\widehat{\rho}(\mathbf{r}) = \rho(O^{-1}\mathbf{r})$: $\nabla^2\widehat{\phi}(\mathbf{r}) = -4\pi\widehat{\rho}(\mathbf{r})$. For notational simplicity we first consider $h \circ i(x)$ for a twice differentiable function $h : R^n \to R$, $i(x) = Ax$ for some $n \times n$ matrix A and representing $x \in R^n$ as a $n \times 1$ column vector in the usual basis. With prime $'$ we denote *the Jacobian matrix*. From calculus we have the generalized chain rule: $(f \circ g)'(a) = f'(g(a))g'(a)$ with $a \in R^p$, and differentiable functions $g : R^p \to R^q$, $f : R^q \to R^r$. Explicit calculation shows that $(Ax)' = A$ and $(x^tA)' = A^t$. Now using the chain rule we can write:

$$\begin{aligned}(h \circ i)'(x) &= h'(i(x))i'(x) = h'(Ax)A\,,\\ (h \circ i)''(x) &= (h'(Ax)A)' = A^t(h'(Ax))' = A^th''(Ax)A\,.\end{aligned}$$

In the usual rectangular coordinates in R^n the Laplacian operator is $\nabla^2 = \sum_{k=1}^n \frac{\partial^2}{\partial x_k^2}$ so we can identify $(\nabla^2 h \circ i)(x)$ as the sum of the diagonal elements or the *trace* Tr of $(h \circ i)''(x)$: $(\nabla^2 h \circ i)(x) = Tr(h \circ i)''(x) = Tr(A^th''(Ax)A)$. The trace operation has the following property for two $n \times n$ matrices A and B: $Tr(AB) = Tr(BA)$, so $(\nabla^2 h \circ i)(x) = Tr(AA^th''(Ax))$. We now see

$$\nabla^2\widehat{\phi}(\mathbf{r}) = Tr(O^{-1}(O^{-1})^t\phi''(O^{-1}\mathbf{r})) = Tr(\phi''(O^{-1}\mathbf{r})) = \nabla^2\phi|_{O^{-1}\mathbf{r}}\,, \tag{6.10}$$

where we used $OO^t = I$ and so $O^{-1} = O^t$ for $O \in$SO(3). We now see that $\nabla^2\widehat{\phi}(\mathbf{r}) = -4\pi\widehat{\rho}(\mathbf{r})$.

Finally we can conclude that successive applications of translations and rotations to a charge distribution and a potential satisfying Poisson's equation result in new solutions to Poisson's equation.

Ritchie and Kemp do in the calculation of the electrostatical energy (6.9) without comment only use the product of ρ_A and ϕ_B together with the product of ρ_B and ϕ_A; but *four* terms are present:

$$\begin{aligned}E &= \frac{1}{2}\int \rho(\mathbf{r})\phi(\mathbf{r})dV = \frac{1}{2}\int (\rho_A(\mathbf{r}) + \rho_B(\mathbf{r}))(\phi_A(\mathbf{r}) + \phi_B(\mathbf{r}))dV\\ &= \frac{1}{2}\int (\rho_A(\mathbf{r})\phi_A(\mathbf{r}) + \rho_B(\mathbf{r})\phi_B(\mathbf{r}))dV + \frac{1}{2}\int (\rho_A(\mathbf{r})\phi_B(\mathbf{r}) + \rho_B(\mathbf{r})\phi_A(\mathbf{r}))dV\,.\end{aligned}$$

However applying translations and rotations to the charge distributions and the potentials leaves the values of $\int \rho_A(\mathbf{r})\phi_A(\mathbf{r})dV$ and $\int \rho_B(\mathbf{r})\phi_B(\mathbf{r})dV$ unchanged; these transformations are bijections and the Jacobian determinant is always 1 ($\det O = 1$). Since the smallest value of E is to be found for different orientations the effective electrostatic energy actually is

$$E_{effective} = \frac{1}{2}\int (\rho_A(\mathbf{r})\phi_B(\mathbf{r}) + \rho_B(\mathbf{r})\phi_A(\mathbf{r}))dV\,. \tag{6.11}$$

The charge distribution corresponding to a collection of *point charges* $\{q_k\}$ located at positions $\{\mathbf{r}_k\}$ can be described using Dirac's delta function $\delta(\mathbf{x})$ in three dimensions:

$$\rho(\mathbf{r}) = \sum_k q_k\delta(\mathbf{r} - \mathbf{r}_k)\,. \tag{6.12}$$

The summation is here, for physical reasons, of course finite. The Dirac delta function is not an actual function but a functional, it can be described consistently within the theory of distributions, the defining equation is $\delta(f) = f(0)$, f a function, (see for example [Rudin, 89] page 141), which more often in the physics literature is written (this formula does not have any meaning in ordinary calculus: "the volume of $\{\mathbf{r} = 0\}$ is 0"):

$$\int f(\mathbf{r})\delta(\mathbf{r})dV = f(0)\,.$$

In this way the Dirac delta function does the job of representing the physics of having charge concentrated at a point. We adopt the physics convention, knowing that the notion can be described consistently.

We apply an expansion as in (6.3) of the charge distribution:

$$\rho = \sum_k q_k \delta_{\mathbf{r}_k} = \sum_{i=1}^{N} c_i^\rho \chi_i \, + \, \xi_N^\rho \,, \tag{6.13}$$

with $c_i^\rho \in R$ and $\xi_N^\rho = \rho - \sum_{i=1}^N c_i^\rho \chi_i$. Again assuming that the (real) functions χ_i, $i = 1, ..., N$ are *orthonormal* with respect to the L^2 - inner product: $< f, g >= \int f(\mathbf{r})\ \overline{g(\mathbf{r})} dV$, we can multiply with χ_j in (6.13) and integrate:

$$\begin{aligned} \sum_k q_k \delta_{\mathbf{r}_k} \chi_j &= \sum_{i=1}^{N} c_i^\rho \chi_i \chi_j + \xi_N^\rho \chi_j \,, \\ \sum_k q_k \chi_j(\mathbf{r}_k) &= c_j^\rho + < \xi_N^\rho, \chi_j > \,, \\ c_j^\rho &= \sum_k q_k \chi_j(\mathbf{r}_k) - < \xi_N^\rho, \chi_j > \,. \end{aligned} \tag{6.14}$$

As mentioned above, in Hex the term corresponding to the ξ_N^ρ-function is neglected. This procedure is carried out for both proteins A and B.

The potential ϕ is also written as an expansion:

$$\phi = \sum_{i=1}^{N} c_i^\phi \chi_i \, + \, \xi_N^\phi \,, \tag{6.15}$$

with $c_i^\phi \in R$ and $\xi_N^\phi = \phi - \sum_{i=1}^N c_i^\phi \chi_i$. The potential ϕ is to be determined from Poisson's equation (6.8), we calculate:

$$\begin{aligned} \nabla^2 \phi(\mathbf{r}) &= -4\pi\rho(\mathbf{r}) \,, \\ \nabla^2 \left(\sum_{i=1}^{N} c_i^\phi \chi_i + \xi_N^\phi \right) &= -4\pi \left(\sum_{i=1}^{N} c_i^\rho \chi_i + \xi_N^\rho \right) \,, \\ \sum_{i=1}^{N} c_i^\phi \nabla^2 \chi_i + \nabla^2 \xi_N^\phi &= -4\pi \sum_{i=1}^{N} c_i^\rho \chi_i - 4\pi \xi_N^\rho \,, \end{aligned}$$

$$\sum_{i=1}^{N} c_i^{\phi}(\nabla^2\chi_i)\chi_j + (\nabla^2\xi_N^{\phi})\chi_j = -4\pi\sum_{i=1}^{N} c_i^{\rho}\chi_i\chi_j - 4\pi\xi_N^{\rho}\chi_j\,,$$

$$\sum_{i=1}^{N} c_i^{\phi} < \nabla^2\chi_i, \chi_j > + < \nabla^2\xi_N^{\phi}, \chi_j > = -4\pi c_j^{\rho} - 4\pi < \xi_N^{\rho}, \chi_j >\,, \tag{6.16}$$

where the functions χ_i, $i = 1, ..., N$ again was assumed to be *orthonormal* with respect to the L^2 - inner product: $< f, g >= \int f(\mathbf{r})\ \overline{g(\mathbf{r})}dV$. With the coefficients c_j^{ρ} known and *neglecting the terms with* ξ_N-functions we see that the c_i^{ϕ}-coefficients can be determined solving a linear system of equations:

$$G\underline{c}^{\phi} = -4\pi\underline{c}^{\rho}\,, \tag{6.17}$$

where $G = (g_{pq})$ is a $N \times N$-matrix with $g_{pq} =< \nabla^2\chi_q, \chi_p >$, $\underline{c}^{\phi}$ is the $N \times 1$-vector of c_q^{ϕ}-coefficients and $\underline{c}^{\rho}$ is the $N \times 1$-vector of c_p^{ρ}-coefficients. The functions χ_i, $i = 1, ..., N$ have to be vanishing at infinity and have vanishing first derivatives at infinity in order to make ϕ a correct solution to Poisson's equation, these properties make it possible to write the following (integration by parts or ∇^2 is self adjoint on an appropriate domain):

$$g_{pq} = \int (\nabla^2\chi_q)(\mathbf{r})\chi_p(\mathbf{r})dV = \int \chi_q(\mathbf{r})(\nabla^2\chi_p)(\mathbf{r})dV =< \nabla^2\chi_p, \chi_q >= g_{qp}\,. \tag{6.18}$$

We see that G is symmetric.

6.3 Scoring Function

Hex uses the following pseudo energy as scoring function:

$$E_{total} = \left(\frac{1391.4}{K_R}\right) E_{effective} + K_H S\,. \tag{6.19}$$

Here S is the shape complementarity score (6.1) and $E_{effective}$ is the part of the classical electrostatic energy which can change with different orientations (6.11), units are in kJ/mol, the relative permittivity K_R and the hydrophobic free energy factor K_H are treated as adjustable parameters. In a testcase ([Ritchie & Kemp, 00] page 185) Ritchie and Kemp used $K_R = 8$ and $K_H = -0.8$ kJ/mol/Å^3. The smallest E_{total} should correspond to the best docking position ($E_{effective}$ is negative and note the negative sign of K_H).

Chapter 7

Radial Functions and Spherical Harmonics

There are several ways to introduce the spherical polar expansions used in Hex. Ritchie and Kemp just specify the expansions used. These expansions use radial functions based on Laguerre-polynomials and the spherical part is controlled by spherical harmonics.

One could take the theory of classical and harmonic polynomials [Erdelyi et al, 53]. Sturm-Liouville theory ([Birkhoff & Rota, 89], [Hinton & Schaefer, 97]) gives the Laguerre-polynomials and the Legendre-polynomials from which the spherical harmonics can be derived. Or maybe introduce the functions as in the work of Andrews, Askey and Roy [Andrews et al, 99] which is based on the gamma function. When considering the spherical harmonics Ritchie and Kemp [Ritchie & Kemp, 00] have reference to a book of Biedenharn and Louck [Biedenharn and Louck, 81] on angular momentum in quantum physics, this book present a group theoretical approach; a short and readable account on the relation between symmetries (Lie groups) and special functions is, among other, given by Dieudonné [Dieudonné, 80].

To give a fast introduction to Laguerre-polynomials and spherical harmonics we can review the solution of the time-independent Schrödinger equation for the hydrogen atom. The expansion used by Ritchie and Kemp does in fact refer to the solution of the Schrödinger equation for the hydrogen atom. We follow [Weissbluth, 78] but instead of taking the theory of angular momentum as a given prerequisite we to some extent develop it for the present purpose, the approach is to solve differential equations; also [Andrews et al, 99] was an important reference.

7.1 The Schrödinger Equation for the Hydrogen Atom

The time-independent, non-relativistic Schrödinger equation for a particle with mass m in a potential V is $H\psi = E\psi$ or

$$\left(-\frac{\hbar^2}{2m}\nabla^2 + V\right)\psi = E\psi, \tag{7.1}$$

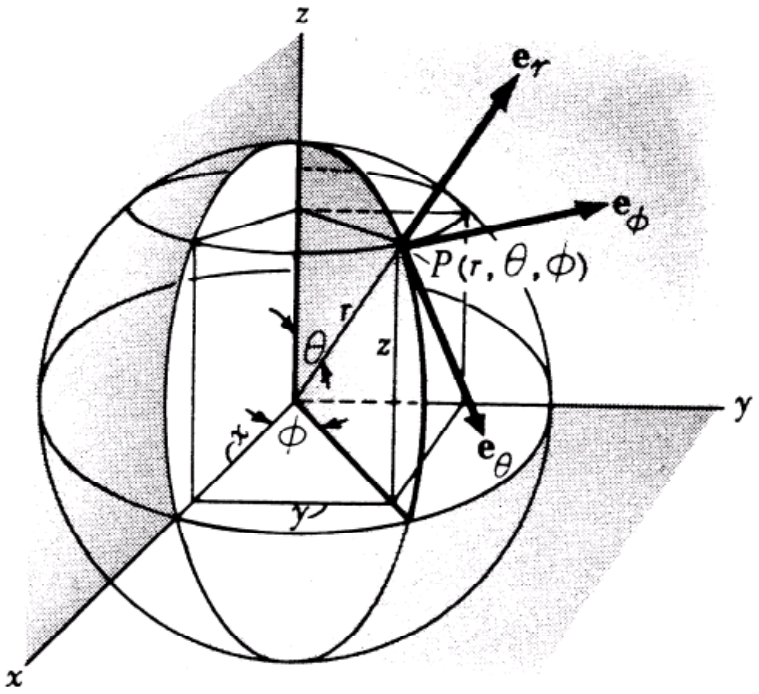

Figure 7.1: [Spiegel, 59] page 138.

where ∇^2 is the Laplacian operator (also denoted Δ) and the real function V acts as a multiplication operator. This equation is also the Schrödinger equation for a two-particle system as seen from the center of mass; then coordinates are for the relative distance $\mathbf{r} = \mathbf{r}_1 - \mathbf{r}_2$ and $m = \frac{m_1 \cdot m_2}{m_1 + m_2}$ is the reduced mass ([Kristensen, 84] page 27.3). The hydrogen atom and hydrogen-like atoms are of course two-particle systems.

The Laplacian operator has the form $\nabla^2 = \frac{\partial^2}{\partial x^2} + \frac{\partial^2}{\partial y^2} + \frac{\partial^2}{\partial z^2}$ in rectangular coordinates x, y, z. Spherical coordinates is (r, θ, ϕ) where $r \geq 0$, $0 \leq \phi < 2\pi$, $0 \leq \theta < \pi$. In spherical coordinates ([Spiegel, 59] page 137 and 154)

$$x = r \sin\theta \cos\phi, \;\; y = r \sin\theta \sin\phi, \;\; z = r \cos\theta$$

and

$$\nabla^2\psi = \frac{1}{r^2}\frac{\partial}{\partial r}\left(r^2\frac{\partial\psi}{\partial r}\right) + \frac{1}{r^2\sin\theta}\frac{\partial}{\partial\theta}\left(\sin\theta\frac{\partial\psi}{\partial\theta}\right) + \frac{1}{r^2\sin^2\theta}\frac{\partial^2\psi}{\partial\phi^2} \tag{7.2}$$

$$= \frac{1}{r^2}\frac{\partial}{\partial r}\left(r^2\frac{\partial\psi}{\partial r}\right) - \frac{1}{r^2}L^2\psi \tag{7.3}$$

in which

$$L^2 = -\left[\frac{1}{\sin\theta}\frac{\partial}{\partial\theta}\left(\sin\theta\frac{\partial}{\partial\theta}\right) + \frac{1}{\sin^2\theta}\frac{\partial^2}{\partial\phi^2}\right]. \tag{7.4}$$

We assume that $V = V(r)$ and

$$\psi(r,\theta,\phi) = \frac{1}{r}P(r)Y(\theta,\phi) = R(r)Y(\theta,\phi)\,.$$

Then the Schrödinger equation (7.1) can be written:

$$\begin{aligned} -\frac{\hbar^2}{2m}\frac{1}{r^2}\frac{\partial}{\partial r}\left(r^2\frac{\partial}{\partial r}\frac{1}{r}P(r)Y(\theta,\phi)\right) + \frac{\hbar^2}{2m}\frac{1}{r^2}L^2\frac{1}{r}P(r)Y(\theta,\phi) & \\ +V(r)\frac{1}{r}P(r)Y(\theta,\phi) &= E\frac{1}{r}P(r)Y(\theta,\phi) \end{aligned}$$

or

$$Y(\theta,\phi)\frac{1}{r}\frac{\partial^2 P(r)}{\partial r^2} - L^2Y(\theta,\phi)\frac{1}{r^3}P(r) + Y(\theta,\phi)\frac{2m}{\hbar^2}\left(E - V(r)\right)\frac{1}{r}P(r) = 0\,.$$

If we divide by $Y(\theta,\phi)\frac{1}{r^3}P(r)$ in this equation (following [Andrews et al, 99] page 448) we get:

$$\frac{r^2}{P(r)}\frac{\partial^2 P(r)}{\partial r^2} + \frac{2mr^2}{\hbar^2}\left(E - V(r)\right) = \frac{L^2Y(\theta,\phi)}{Y(\theta,\phi)}\,.$$

This equation can only be true if there exist a constant λ, a separation constant, so that:

$$\begin{aligned} \frac{r^2}{P(r)}\frac{\partial^2 P(r)}{\partial r^2} + \frac{2mr^2}{\hbar^2}\left(E - V(r)\right) &= \lambda\,, \\ \frac{L^2Y(\theta,\phi)}{Y(\theta,\phi)} &= \lambda \end{aligned}$$

or

$$\frac{d^2P(r)}{dr^2} + \frac{2m}{\hbar^2}\left(E - V(r)\right)P(r) = \frac{\lambda}{r^2}P(r)\,, \tag{7.5}$$

$$L^2Y(\theta,\phi) = \lambda Y(\theta,\phi)\,. \tag{7.6}$$

We now first consider (7.6) which will give rise to the spherical harmonics and afterwards we consider (7.5).

7.1.1 Spherical Harmonics, Separation of Differential Equation

Equation (7.6) can be written

$$-\frac{1}{\sin\theta}\frac{\partial}{\partial\theta}\left(\sin\theta\frac{\partial Y(\theta,\phi)}{\partial\theta}\right) - \frac{1}{\sin^2\theta}\frac{\partial^2 Y(\theta,\phi)}{\partial\phi^2} = \lambda Y(\theta,\phi)\,.$$

We write $Y(\theta,\phi) = T(\theta)F(\phi)$ and try to separate ([Andrews et al, 99] page 448) this equation in two:

$$-\frac{F(\phi)}{\sin\theta}\frac{\partial}{\partial\theta}\left(\sin\theta\frac{\partial T(\theta)}{\partial\theta}\right) - \frac{T(\theta)}{\sin^2\theta}\frac{\partial^2 F(\phi)}{\partial\phi^2} = \lambda T(\theta)F(\phi)\,,$$

division by $T(\theta)F(\phi)$ gives

$$-\frac{1}{T(\theta)\sin\theta}\frac{\partial}{\partial\theta}\left(\sin\theta\frac{\partial T(\theta)}{\partial\theta}\right)-\frac{1}{F(\phi)\sin^2\theta}\frac{\partial^2F(\phi)}{\partial\phi^2}=\lambda\,,$$

or

$$\frac{\sin\theta}{T(\theta)}\frac{\partial}{\partial\theta}\left(\sin\theta\frac{\partial T(\theta)}{\partial\theta}\right)+\lambda\sin^2\theta=-\frac{1}{F(\phi)}\frac{\partial^2F(\phi)}{\partial\phi^2}\,.$$

We conclude that there must exist a separation constant μ such that

$$\begin{aligned}\frac{\sin\theta}{T(\theta)}\frac{d}{d\theta}\left(\sin\theta\frac{dT(\theta)}{d\theta}\right)+\lambda\sin^2\theta &= \mu\,,\\ -\frac{1}{F(\phi)}\frac{d^2F(\phi)}{d\phi^2} &= \mu\,,\end{aligned}$$

or

$$\frac{1}{\sin\theta}\frac{d}{d\theta}\left(\sin\theta\frac{dT(\theta)}{d\theta}\right)+\left(\lambda-\frac{\mu}{\sin^2\theta}\right)T(\theta) = 0\,, \tag{7.7}$$

$$\frac{d^2F(\phi)}{d\phi^2}+\mu F(\phi) = 0\,. \tag{7.8}$$

We first consider (7.7). Set $T(\theta)=u(\cos\theta)$ and let prime $'$ denote differentiation, then

$$\frac{d}{d\theta}\left(\sin\theta\frac{dT(\theta)}{d\theta}\right)=\frac{d}{d\theta}\left(-\sin^2\theta u'(\cos\theta)\right)=-2\sin\theta\cos\theta u'(\cos\theta)+\sin^3\theta u''(\cos\theta)\,.$$

Now with $t=\cos\theta$ we see that (7.7) can be written

$$(1-t^2)\frac{d^2u}{dt^2}-2t\frac{du}{dt}+\left(\lambda-\frac{\mu}{1-t^2}\right)u=0\,, \tag{7.9}$$

or

$$\frac{d}{dt}\left((1-t^2)\frac{du}{dt}\right)+\left(\lambda-\frac{\mu}{1-t^2}\right)u=0\,. \tag{7.10}$$

Equation (7.10) is the *associated Legendre equation* ([Talman, 68] page 166, with $\mu=m^2$). For $\mu=0$ the equation is called the Legendre equation (see for example [Birkhoff & Rota, 89] page 34). We now return to the radial equation (7.5) to see if we can get some information about λ.

7.1.2 Radial Functions, Differential Equation

If we impose the requirement

$$V(r)\to 0 \quad as \quad r\to\infty$$

then the radial differential equation (7.5) can be approximated with the following differential equation for large values of r

$$\frac{d^2P(r)}{dr^2} + \frac{2m}{\hbar^2}EP(r) = 0\,,$$

which, introducing the parameter $a = \sqrt{-\frac{2mE}{\hbar^2}}$, has the solutions

$$P(r) = ce^{\pm ar}\,,$$

with c a constant.

If $E > 0$ the parameter a is complex and $P(r) = ce^{\pm ar}$ is bound and oscillating: a possible solution (scattering states). We will not discuss the $E > 0$ case any further.

If $E < 0$ the parameter a is real and positive. The solution $P(r) = ce^{ar}$ grows to infinity for $r \to \infty$; this is a non-physical solution, the quantum mechanical wavefunction $\psi(r,\theta,\phi) = \frac{1}{r}P(r)Y(\theta,\phi)$ has to be bound (and appropriate smooth) for physical reasons. On the other hand $ce^{-ar} \to 0$ for $r \to \infty$ and we are led to the ansatz $P(r) = e^{-ar}f(r)$. In other words we were led to the common trick of applying an exponential multiplier.

To proceed further we have to specify the form of the potential $V(r)$. For hydrogen ($Z = 1$) and hydrogen-like atoms is

$$V(r) = -\frac{Ze^2}{r}\,,$$

and our differential equation of concern (7.5) becomes

$$\frac{d^2P(r)}{dr^2} + \frac{2m}{\hbar^2}\left(E + \frac{Ze^2}{r} - \frac{\lambda}{r^2}\right)P(r) = 0\,. \tag{7.11}$$

We now insert $P(r) = e^{-ar}f(r)$ into (7.11):

$$\begin{aligned}\frac{d^2e^{-ar}f(r)}{dr^2} + \frac{2m}{\hbar^2}\left(E + \frac{Ze^2}{r} - \frac{\lambda}{r^2}\right)e^{-ar}f(r) &= 0\,,\\ \frac{d^2f}{dr^2} - 2a\frac{df}{dr} + a^2f + \frac{2m}{\hbar^2}\left(E + \frac{Ze^2}{r} - \frac{\lambda}{r^2}\right)f(r) &= 0\,.\end{aligned}$$

We see that $a^2f + \frac{2mE}{\hbar^2}f = 0$ with the above definition of the parameter a and therefore:

$$\frac{d^2f}{dr^2} - 2a\frac{df}{dr} + \frac{2m}{\hbar^2}\left(\frac{Ze^2}{r} - \frac{\lambda}{r^2}\right)f(r) = 0\,.$$

Multiplying in this equation with a_o^2, where $a_o = \frac{\hbar^2}{me^2}$ =0.5292 Å is the Bohr radius, transforms the equation into the following equation with r in units of a_o:

$$\frac{d^2f}{dr^2} - 2\tilde{a}\frac{df}{dr} + \left(\frac{2Z}{r} - \frac{\lambda}{r^2}\right)f = 0\,, \tag{7.12}$$

where $\tilde{a} = \sqrt{\frac{-E}{R_\infty}}$ and $R_\infty = \frac{1}{2}mc^2(\frac{e^2}{\hbar c})^2 = \frac{me^4}{2\hbar^2}$=13.605 eV is the Rydberg constant.

Power Series

In order to solve (7.12) we try a power series solution: $f(r) = \sum_{k=0}^{\infty} A_k r^k$; within the radius of convergence we can differentiate it term by term. Not every function can be represented as a power series but it works here and for example is it easy to see that functions $r \to \frac{1}{r^s}$, s positive, are not solutions to (7.12). A more systematic approach using hypergeometric series (series $\sum c_n$ where $\frac{c_{n+1}}{c_n}$ is a rational function of n) and hypergeometric functions is given in [Kristensen, 84] and [Andrews et al, 99].

Note that we do not specify any boundary conditions for (7.12) and therefore we will not get a unique solution. This is a part of the game: we find the eigenspaces of solutions corresponding to different eigenvalues. Actually Weissbluth talks about that "*the boundary conditions have forced the bound states to be discrete*" (with reference to (7.18) below, [Weissbluth, 78] page 325). He apparently considers the requirement that P can not grow exponentially to infinity as $r \to \infty$, which we also used above, as a boundary condition. Strictly, this is not a boundary condition, this is a condition stated because the wavefunction ψ has to be square-integrable: the quantum mechanical function space is the Hilbert space $L^2(R^3)$.

Now we proceed to solve (7.12). With the above ansatz we have $\frac{df}{dr} = \sum_{k=0}^{\infty} k A_k r^{k-1}$ and $\frac{d^2 f}{dr^2} = \sum_{k=0}^{\infty} k(k-1) A_k r^{k-2}$ which we insert in (7.12):

$$\begin{aligned} \sum_{k=0}^{\infty} k(k-1) A_k r^{k-2} - 2\tilde{a} \sum_{k=0}^{\infty} k A_k r^{k-1} + \left(\frac{2Z}{r} - \frac{\lambda}{r^2} \right) \sum_{k=0}^{\infty} A_k r^k &= 0\,, \\ \sum_{k=0}^{\infty} k(k-1) A_k r^{k-2} - 2\tilde{a} \sum_{k=0}^{\infty} k A_k r^{k-1} + \sum_{k=0}^{\infty} 2Z A_k r^{k-1} - \sum_{k=0}^{\infty} \lambda A_k r^{k-2} &= 0\,. \end{aligned}$$

Arranging terms according to powers $k-1$ and $k-2$ of r

$$\sum_{k=0}^{\infty} \left(k(k-1) - \lambda \right) A_k r^{k-2} + \sum_{k=0}^{\infty} \left(2Z - 2\tilde{a}k \right) A_k r^{k-1} = 0\,.$$

Here we have to be careful. We see that necessarily $A_0 = 0$ (or $k(k-1) - \lambda = 0$ for $k = 0$) due to the corresponding r^{-2} factor in the first summation. It is of course possible that $A_0 = A_1 = ... = A_l = 0$ with A_{l+1} as the first non-zero coefficient for some integer $l \geq 0$, therefore:

$$\sum_{k=l+1}^{\infty} \left(k(k-1) - \lambda \right) A_k r^{k-2} + \sum_{k=l+1}^{\infty} \left(2Z - 2\tilde{a}k \right) A_k r^{k-1} = 0\,,$$

or

$$\left((l+1)l - \lambda \right) A_{l+1} r^{l-1} + \sum_{k=l+1}^{\infty} \left((k+1)k - \lambda \right) A_{k+1} r^{k-1} + \sum_{k=l+1}^{\infty} \left(2Z - 2\tilde{a}k \right) A_k r^{k-1} = 0\,,$$

and finally

$$\left((l+1)l - \lambda \right) A_{l+1} r^{l-1} + \sum_{k=l+1}^{\infty} \left[\left((k+1)k - \lambda \right) A_{k+1} + \left(2Z - 2\tilde{a}k \right) A_k \right] r^{k-1} = 0\,. \qquad (7.13)$$

From this equation we get the well-known result

$$\lambda = l(l+1)\,, \tag{7.14}$$

and

$$((k+1)k - \lambda)\,A_{k+1} + 2\,(Z - \tilde{a}k)\,A_k = 0\,, \quad k = l+1, l+2, ...; \tag{7.15}$$

this last equation gives the *recurrence relation*

$$A_{k+1} = \frac{2\,(\tilde{a}k - Z)}{(k+1)k - \lambda} A_k\,, \quad k = l+1, l+2, ... \tag{7.16}$$

From (7.16) we find

$$\frac{A_{k+1}}{A_k} \approx \frac{2\tilde{a}}{k+1} \quad as\, k \to \infty\,.$$

Comparing the series $f(r) = \sum_{k=0}^{\infty} A_k r^k$ with the exponential series $\exp(x) = \sum_{k=0}^{\infty} \frac{x^k}{k!}$ we see that $f(r) \approx e^{2\tilde{a}r}$ for large r; note here that r is measured in units of the Bohr radius a_o. Because $ar = aa_o\frac{r}{a_o} = \tilde{a}\frac{r}{a_o}$ this has the following consequence with r measured in units of a_o:

$$P(r) = e^{-\tilde{a}r} f(r) \approx e^{-\tilde{a}r} e^{2\tilde{a}r} = e^{\tilde{a}r} \quad as\, k \to \infty\,,$$

again this gives an unbound wavefunction which is not a physical solution. Therefore we have to truncate the series for f so that $A_{n+1} = A_{n+2} = ... = 0$ and with A_n as last non-zero coefficient for some integer $n > l$. Comparing with (7.15) we see

$$Z - \tilde{a}n = 0\,, \tag{7.17}$$

and because $\tilde{a} = \sqrt{\frac{-E}{R_\infty}}$ we have the celebrated formula for the energy-levels in hydrogen-like atoms:

$$E = -\frac{Z^2}{n^2} R_\infty\,. \tag{7.18}$$

Due to 7.14 and (7.17) we can rewrite the recurrence relation (7.16):

$$A_{k+1} = -2\tilde{a}\frac{n-k}{(k+1)k - l(l+1)} A_k \quad , k = l+1, l+2, ..., n-1\,. \tag{7.19}$$

With the above considerations introducing l and n we have $f(r) = \sum_{k=0}^{\infty} A_k r^k = \sum_{k=l+1}^{n} A_k r^k$, or changing the index of summation to i $(k = l+1+i)$: $f(r) = r^{l+1} \sum_{i=0}^{n-(l+1)} A_{l+1+i} r^i$. Renaming A_{l+1+i} to $2\tilde{a}B_i$ we can write

$$f(r) = r^{l+1} \sum_{i=0}^{n-(l+1)} B_i (2\tilde{a}r)^i\,. \tag{7.20}$$

Now the recurrence relation reads

$$B_{i+1} = -\frac{n-(l+1+i)}{(l+2+i)(l+1+i) - l(l+1)} B_i \quad , i = 0, 1, ..., n-(l+1)\,,$$

or maybe a bit more readable

$$B_i = -\frac{n-(l+i)}{(l+1+i)(l+i) - l(l+1)} B_{i-1} \quad , i = 1, ..., n-l\,. \tag{7.21}$$

Recurrence Relation

If we compare with formula (A6-2) page 692 in Weissbluth's book [Weissbluth, 78] the following recurrence formula for the coefficients in a L_{n+l}^{2l+1}-Laguerre polynomial is presented:

$$B_i = -B_{i-1}\frac{n-l-i}{i(2l+i+1)}\,.$$

The denominator in our relation (7.21) is

$$(l+1+i)(l+i) - l(l+1) = i(2l+1+i)\,,$$

and therefore the two recurrence relations are the same.

We can also compare with formula (C.7) page 119 in Ritchie's Ph.D. thesis [Ritchie, 98] giving the *normalized* Laguerre polynomials L_p^q:

$$L_p^q(\rho) = \sum_{k=0}^{p-q}\frac{(-1)^{k+q}\sqrt{(p-q)!p!}}{(p-q-k)!(k+q)!k!}\rho^k\,. \tag{7.22}$$

With $p = n+l$ and $q = 2l+1$ we calculate the fraction B_k/B_{k-1} between the coefficients of ρ^k and ρ^{k-1} in (7.22):

$$\begin{aligned}\frac{B_k}{B_{k-1}} &= -\frac{(n+l-(2l+1)-(k-1))!(k-1+2l+1)!(k-1)!}{(n+l-(2l+1)-k)!(k+2l+1)!k!}\\ &= -\frac{n-l-k}{(k+2l+1)k}\,;\end{aligned}$$

again in agreement with our result.[1] Also note that the upper limit of summation in (7.22) is $p-q$, which is equal to $n-(l+1)$ as in (7.20) for $p = n+l$ and $q = 2l+1$.

The Radial Functions

Apart from a constant factor the recurrence relation uniquely determines the polynomials. We conclude that

$$P(r) = e^{-\widetilde{a}r}f(r) = e^{-\widetilde{a}r}r^{l+1}f(r) = e^{-\widetilde{a}r}r^{l+1}L_{n+l}^{2l+1}(2\widetilde{a}r)\,,$$

non-normalized, with r in units of Bohr radius a_o and $\widetilde{a} = \sqrt{\frac{-E}{R_\infty}}$, $E = -\frac{Z^2}{n^2}R_\infty$. We get $\widetilde{a} = \frac{Z}{n}$ and writing the Bohr radius explicitly we can state our result as

$$P_{nl}(r) = N_{nl}e^{-Zr/(na_o)}(\frac{2Zr}{na_0})^{l+1}L_{n+l}^{2l+1}(2\widetilde{a}r)\,, \tag{7.23}$$

[1] The same agreement did not come through in a first calculation when using formula (7) page 188 of [Erdelyi et al, 53] or formula (6.2.2) page 283 in [Andrews et al, 99] for the Laguerre polynomials L_n^α; these two formulas on the Laguerre polynomials coincide.

where N_{nl} is a normalization constant. This is in agreement with formula (16.1-32) page 327 in Weissbluth's book [Weissbluth, 78]:

$$P_{nl}(r) = \sqrt{\frac{(n-l-1)!Z}{n^2[(n+l)!]^3 a_o}}(\frac{2Zr}{na_0})^{l+1}e^{-Zr/(na_o)}L_{n+l}^{2l+1}(2\tilde{a}r)\,; \tag{7.24}$$

in this formula the normalization constant is included, because according to Weissbluth ([Weissbluth, 78] page 327):

$$\int_0^\infty P_{nl}(r)P_{n'l}(r)dr = \delta_{nn'}\,.$$

Note that this normalization gives the corresponding normalization

$$\int_0^\infty R_{nl}(r)R_{n'l}(r)r^2dr = \delta_{nn'}$$

of the R_{nl}-functions: $R(r) = \frac{1}{r}P(r)$. This is as wanted because the volume element in spherical coordinates is $dV = r^2\sin\theta dr d\theta d\phi$.

7.1.3 Spherical Harmonics, Differential Equation

We have $\lambda = l(l+1)$ for l a non-negative integer and now we try to solve for the angular part $Y(\theta,\phi) = T(\theta)F(\phi)$ for which we derived (7.7) and (7.8). Equation (7.7) gave (7.10) which we now consider for $\mu = 0$. With the ansatz $u = \sum_{i=0}^\infty C_i t^i$ we have

$$\begin{aligned}\frac{d}{dt}\left((1-t^2)\frac{du}{dt}\right) &= \frac{d}{dt}\left((1-t^2)\sum_{i=0}^\infty C_i i t^{i-1}\right) = \frac{d}{dt}\left(\sum_{i=0}^\infty C_i i t^{i-1} - \sum_{i=0}^\infty C_i i t^{i+1}\right)\,,\\ &= \sum_{i=0}^\infty C_i i(i-1)t^{i-2} - \sum_{i=0}^\infty C_i i(i+1)t^i\,.\end{aligned}$$

For $\mu = 0$ (7.10) is then

$$\sum_{i=0}^\infty C_i i(i-1)t^{i-2} - \sum_{i=0}^\infty C_i i(i+1)t^i + \lambda\sum_{i=0}^\infty C_i t^i = 0\,,$$

or if we collect terms according to powers of t

$$\sum_{i=0}^\infty \left[C_{i+2}(i+2)(i+1) - C_i(i(i+1)-\lambda)\right]t^i = 0\,,$$

and we get the following recurrence relation

$$C_{i+2} = \frac{i(i+1)-\lambda}{(i+2)(i+1)}C_i\,. \tag{7.25}$$

But $\lambda = l(l+1)$ for some nonnegative integer l; from (7.25) we see that the series will terminate for $i = l$ leaving a polynomial solution: the *Legendre polynomial* P_l. If l is even the polynomial consists of even powers of t and the polynomial will be an even function; if l is odd the polynomial consists of odd powers of t and the polynomial will be an odd function ([Birkhoff & Rota, 89] page 102).

For $\mu \neq 0$ (7.10) becomes more difficult to solve. If one substitutes a power series $u = \sum_{i=0}^{\infty} C_i t^i$ into (7.9) the result is (multiply with $(1-t^2)$ in (7.9)) a recurrence relation between coefficients C_{i-2}, C_i and C_{i+2}, this is not easy to deal with.

Solutions to (7.10) are actually the *associated Legendre functions* P_l^m, where $\mu = m^2$ for integer m: $0 \leq m \leq l$ ([Talman, 68] page 164 and 166):

$$P_l^m(t) = \frac{(1-t^2)^{m/2}}{2^l l!} \frac{d^{l+m}}{dt^{l+m}} (t^2-1)^l \,. \tag{7.26}$$

Ritchie has included a phase factor $(-1)^m$ in the expression for P_l^m ([Ritchie, 98] formula (B.9) page 112). We see that for even m the P_l^m functions are polynomials, but for odd m the P_l^m functions are *not* polynomials but polynomials multiplied with $\sqrt{1-t^2}$. (Ritchie does a bit misleading talk about the associated Legendre polynomials, [Ritchie, 98] page 111-113.) With this hindsight we try to solve (7.10) using the transformation $u(t) = u(z(t))$, where $z^2 = 1-t^2$. Note that we consider (7.10) on the interval with endpoints -1 and 1 (because $t = \cos\theta$) where $1-t^2$ is non-negative. We let prime ' denote differentiation with respect to t and calculate: $2zz' = -2t$ or $z' = -t/z$ and

$$\begin{aligned}
\left(\lambda - \frac{\mu}{1-t^2}\right) u &= \left(\lambda - \frac{\mu}{z^2}\right) u \,, \\
\frac{du}{dt} &= \frac{du}{dz}\frac{dz}{dt} = -\frac{t}{z}\frac{du}{dz} \,, \\
-2t\frac{du}{dt} &= 2\frac{t^2}{z}\frac{du}{dz} = 2\frac{1-z^2}{z}\frac{du}{dz} \,, \\
\frac{d^2u}{dt^2} &= -\frac{z-tz'}{z^2}\frac{du}{dz} - \frac{t}{z}\frac{d^2u}{dz^2}z' = \frac{t^2}{z^2}\frac{d^2u}{dz^2} - \left(\frac{1}{z} + \frac{t^2}{z^3}\right)\frac{du}{dz} \,, \\
(1-t^2)\frac{d^2u}{dt^2} &= (1-z^2)\frac{d^2u}{dz^2} - \left(z + \frac{1-z^2}{z}\right)\frac{du}{dz} \,.
\end{aligned}$$

We insert into (7.9):

$$(1-z^2)\frac{d^2u}{dz^2} - \left(z + \frac{1-z^2}{z}\right)\frac{du}{dz} + 2\frac{1-z^2}{z}\frac{du}{dz} + \left(\lambda - \frac{\mu}{z^2}\right) u = 0 \,,$$

or

$$(1-z^2)\frac{d^2u}{dz^2} + \left(\frac{1}{z} - 2z\right)\frac{du}{dz} + \left(\lambda - \frac{\mu}{z^2}\right) u = 0 \,. \tag{7.27}$$

We again use a power series ansatz, $u(z) = \sum_{j=0}^{\infty} D_j z^j$, and insert into (7.27):

$$(1-z^2)\sum_{j=0}^{\infty} j(j-1) D_j z^{j-2} + \left(\frac{1}{z} - 2z\right)\sum_{j=0}^{\infty} j D_j z^{j-1} + \left(\lambda - \frac{\mu}{z^2}\right)\sum_{j=0}^{\infty} D z^j = 0 \,,$$

or collecting terms according to the different powers of z:

$$\sum_{j=0}^{\infty} (j(j-1)+j-\mu)\, D_j z^{j-2} + \sum_{j=0}^{\infty} (\lambda - j(j-1) - 2j)\, D_j z^j = 0\,,$$

or

$$\sum_{j=0}^{\infty} \left(j^2-\mu\right) D_j z^{j-2} + \sum_{j=0}^{\infty} (\lambda - j(j+1))\, D_j z^j = 0\,. \tag{7.28}$$

We recognize some similarity with the expressions we derived when we solved the radial equation. We see that necessarily $D_0 = D_1 = 0$ (or $j^2 - \mu = 0$ for $j = 0, 1$) due to the corresponding z^{-2} and z^{-1} factors. It is possible that $D_0 = D_1 = ... = D_{m-1} = 0$ with D_m as the first non-zero coefficient for some integer $m \geq 0$, then $(m^2 - \mu)\, D_m z^{m-2} = 0$ or $\mu = m^2$. The result

$$\mu = m^2 \tag{7.29}$$

for some integer $m \geq 0$ is the expected, and probably one could get $m \leq l$ too (notice the $(\lambda - j(j+1))\, D_j$ coefficient in the second series of (7.28), it is zero for $j = l$ because $\lambda = l(l+1)$). We will not elaborate more on (7.28) but state that

$$T(\theta) = P_l^m(\cos\theta)\,, \quad 0 \leq m \leq l\,,$$

where P_l^m are the associated Legendre functions and m, l are integers. Negative, integer m are allowed, negative m will not alter the differential equation (7.7) for $T(\theta)$ because it is $\mu = m^2$ which enters the equation; one let $P_l^m = (-1)^m P_l^{|m|}$ for negative m. ([Ritchie, 98] (B.12) page 113 or [Weissbluth, 78] (1.2-3a) page 5; note, different phase conventions exist).

We now consider the differential equation (7.8) for F with $\mu = m^2$:

$$\frac{d^2F(\phi)}{d\phi^2} + m^2 F(\phi) = 0\,.$$

The solution to this equation is of course $F(\phi) = e^{im\phi}$ (with constants of integration conveniently chosen).

We can now state that

$$Y(\theta,\phi) = C_{lm} P_l^m(\cos\theta) e^{im\phi}\,, \tag{7.30}$$

where C_{lm} is an appropriate phase and normalization constant. Formula (1.2-1) page 3 in Weissbluth's book [Weissbluth, 78] specify the *spherical harmonics* as

$$Y_{lm}(\theta,\phi) = \sqrt{(-1)^{m+|m|}}\sqrt{\frac{2l+1}{4\pi}}\sqrt{\frac{(l-|m|)!}{(l+|m|)!}} P_l^{|m|}(\cos\theta) e^{im\phi}\,, \tag{7.31}$$

the phase convention here chosen is known as the *Condon-Shortley convention* and the normalization factor gives the following orthonormality relation ([Weissbluth, 78] page 5):

$$\int Y_{lm}(\theta,\phi)\overline{Y_{l'm'}(\theta,\phi)} \sin\theta d\theta d\phi = \delta_{ll'}\delta_{mm'}\,, \tag{7.32}$$

we recognize the angular part $d\Omega = \sin\theta d\theta d\phi$ of the volume element $dV = r^2 \sin\theta dr d\theta d\phi$ in spherical coordinates.

7.1.4 The Solution

In conclusion we state although we not have covered every detail that the solution to the time-independent Schrödinger equation (7.1) with the Coulomb potential $V(r) = \frac{-Ze^2}{r}$(hydrogen-like atoms) for $E < 0$ in spherical coordinates is:

$$\psi_{nlm}(r,\theta,\phi) = R_{nl}(r)Y_{lm}(\theta,\phi)\,, \tag{7.33}$$

where the radial functions R_{nl} are given by (7.24) and the spherical harmonics $Y_{lm}(\theta,\phi)$ are given by (7.31). The solutions satisfy the orthogonality relation:

$$\int \psi_{nlm}(r,\theta,\phi)\psi_{n'l'm'}(r,\theta,\phi)dV = \delta_{nn'}\delta_{ll'}\delta_{mm'}\,,$$

where $dV = r^2\sin\theta dr d\theta d\phi$ is the volume element in spherical coordinates.

7.2 Spherical Polar Expansions

Ritchie and Kemp use two different spherical polar expansions according to if the expansions are used to represent *surface skins* or *electrostatic potentials*. In both cases the expansions of a function $f(\mathbf{r})$ can be written as ([Ritchie & Kemp, 00] page 180):

$$f_N(\mathbf{r}) = \sum_{nlm}^{N} a_{nlm}T_{nl}(r)y_{lm}(\theta,\phi)\,, \quad N \geq n > l \geq |m| \geq 0, \tag{7.34}$$

where a_{nlm} are the expansion coefficients, the radial functions T_{nl} differ according to if skins or potentials are expanded, and y_{lm} are the *real* spherical harmonics. The indices are integers and for clarity we state that the m-indices are $l, l-1, ..., 0, ..., -l$. The expansion coefficients a_{nlm} are calculated as (real functions):

$$a_{nlm} =< f,\, T_{nl}y_{lm} >= \int f(\mathbf{r})T_{nl}(r)y_{lm}(\theta,\phi)dV\,.$$

For surface skins the following radial functions are used ([Ritchie & Kemp, 00] page 180):

$$S_{nl}(r) = \left[\left(\frac{2}{k^{\frac{3}{2}}}\right)\frac{(n-l-1)!}{\Gamma(n+\frac{1}{2})}\right]^{\frac{1}{2}} e^{-\frac{\rho}{2}}\rho^{\frac{l}{2}}L_{n-l-1}^{l+\frac{1}{2}}(\rho)\,, \tag{7.35}$$

where ρ is a scaled distance: $\rho = \frac{r^2}{k}$, with scaling factor $k = 20$, and Γ is the gamma function.

Electrostatic potentials are represented using ([Ritchie & Kemp, 00] page 180) the following radial functions:

$$V_{nl}(r) = \left[(2\Lambda)^3\frac{(n-l-1)!}{(n+l+1)!}\right]^{\frac{1}{2}} e^{-\frac{\rho}{2}}\rho^{l}L_{n-l-1}^{2l+2}(\rho)\,, \tag{7.36}$$

where $\rho = 2\Lambda r$, with scale factor $\Lambda = \frac{1}{2}$.

We recognize the similarity of the functions $T_{nl}y_{lm}$, where $T_{nl} = S_{nl}$ for surface skins and $T_{nl} = V_{nl}$ for electrostatic potentials, with the solutions of the Schrödinger equation (7.33). Instead of the spherical harmonics Y_{lm} real spherical harmonics y_{lm} are used, this is of course no significant change, a decaying exponential is again present and the independent variable to some power is a factor. The difference is the use of different associated Laguerre polynomials L_q^α and the scaling. Ritchie do in his Ph.D.-thesis in fact take outset in the radial functions from the solution of the Schrödinger equation, but the mean value of the R_{nl} radial functions increases as n^2 which not is desirable in protein shape parametrisations ([Ritchie, 98] page 59). Ritchie then considers different associated Laguerre polynomials and different types of scaling before he states the radial functions he wants to use for the spherical expansion of the surface skins ([Ritchie, 98] formula (6.13) page 62). Apparently the radial functions found *is not* the one stated in [Ritchie & Kemp, 00] and which is reproduced in (7.35): the scaling uses $\rho = \frac{1}{3}(\frac{r}{r_0})^3$ and the Laguerre polynomials have different indices. (The different indices in the Laguerre polynomials could of course also be due to different usage of notation; the references to the Laguerre polynomials in [Ritchie, 98] are [Hobson, 31] and [Pauling & Wilson, 35], whereas it is [Erdelyi et al, 53] in [Ritchie & Kemp, 00].)

In the next section we consider the orthonormality of the radial functions.

7.3 Associated Laguerre Polynomials

Ritchie and Kemp give [Erdelyi et al, 53] as reference to the generalized Laguerre polynomials. In equation (41) page 185 of [Ritchie & Kemp, 00] they state

$$L_q^\alpha(\rho) = \sum_{k=0}^{q} \left(\begin{array}{c} q+\alpha \\ q-\alpha \end{array} \right) \frac{(-\rho)^k}{k!} ;$$

this equation is the same as equation (7) page 188 in [Erdelyi et al, 53]. We can rely on that [Erdelyi et al, 53] is the correct reference for the associated Laguerre polynomials.

The reference [Erdelyi et al, 53] and the reference [Andrews et al, 99] do agree on the associated Laguerre polynomials. In [Andrews et al, 99] ((6.2.3) page 283) the following formula containing the orthogonality relation for the associated Laguerre polynomials is given

$$\int_0^\infty L_m^\alpha(x) L_n^\alpha(x) x^\alpha e^{-x} dx = \frac{\Gamma(\alpha+n+1)}{n!}\delta_{mn} , \quad \alpha > -1 , \tag{7.37}$$

where Γ is the gamma-function. We now show the orthonormality of the radial functions (7.35) with respect to r^2dr, note l is the same for both radial functions, orthonormality for different l is mediated through the spherical harmonics:

$$\begin{aligned} \int_0^\infty S_{n'l}(r) S_{nl}(r) r^2 dr &= \int_0^\infty C_{n'l} e^{-\frac{\rho}{2}} \rho^{\frac{l}{2}} L_{n'-l-1}^{l+\frac{1}{2}}(\rho) C_{nl} e^{-\frac{\rho}{2}} \rho^{\frac{l}{2}} L_{n-l-1}^{l+\frac{1}{2}}(\rho) r^2 dr \\ &= C_{n'l} C_{nl} \int_0^\infty L_{n'-l-1}^{l+\frac{1}{2}}(\rho) L_{n-l-1}^{l+\frac{1}{2}}(\rho) e^{-\rho} \rho^l r^2 dr \end{aligned}$$

$$
\begin{aligned}
&= C_{n'l}C_{nl}\frac{k^{\frac{3}{2}}}{2}\int_0^\infty L_{n'-l-1}^{l+\frac{1}{2}}(\rho)L_{n-l-1}^{l+\frac{1}{2}}(\rho)e^{-\rho}\rho^{l+\frac{1}{2}}d\rho \\
&= \left[\left(\frac{2}{k^{\frac{3}{2}}}\right)\frac{(n'-l-1)!}{\Gamma(n'+\frac{1}{2})}\right]^{\frac{1}{2}}\left[\left(\frac{2}{k^{\frac{3}{2}}}\right)\frac{(n-l-1)!}{\Gamma(n+\frac{1}{2})}\right]^{\frac{1}{2}}\frac{k^{\frac{3}{2}}}{2} \\
&\qquad\qquad \times\frac{\Gamma(l+\frac{1}{2}+n-l-1+1)}{(n-l-1)!}\delta_{n'n} \\
&= \delta_{n'n}\,.
\end{aligned}
$$

The orthonormality of the radial functions (7.36) with respect to r^2dr is left to the reader.

The functions $\{T_{nl}y_{lm}\}_{nlm}$ used in (7.34) do not form a complete orthonormal basis set of $L^2(R^3)$. The orthonormality is satisfied and the real spherical harmonics $\{y_{lm}\}_{lm}$ do form a complete set on the sphere but the associated Laguerre functions L_n^α used in the expressions (7.35) and (7.36) only form complete sets (α constant) in $L^2([0,\infty[\,,x^ae^{-x}dx)$. A proof using Fourier-transform methods and complex function theory of this can be found in [Andrews et al, 99] pages 306-309. If we compare with our solution of the Schrödinger equation (noting that this equation is an eigenvalue equation for a self-adjoint operator and referring to spectral theory) we already could have remarked this: we did only consider negative energy values of E and not non-negative values of E. In practice this is not necessarily a problem due to the finiteness of the molecules and the decay of the potentials.

7.4 Spherical Harmonics

The real spherical harmonics $\{y_{lm}\}_{lm}$ are obtained from the complex spherical harmonics $\{Y_{lm}\}_{lm}$ (7.31) the usual way (though, some care has to be taken with the values of m, [Ritchie & Kemp, 99] page 386):

$$
y_{lm}(\theta,\phi) = \begin{cases} (Y_{lm}(\theta,\phi)+\overline{Y_{lm}(\theta,\phi)})/\sqrt{2} & if\ m>0 \\ Y_{l0}(\theta,\phi) \quad if\ m=0 \\ -i(Y_{l|m|}(\theta,\phi)-\overline{Y_{l|m|}(\theta,\phi)})/\sqrt{2} & if\ m<0 \end{cases}
$$

There is no ambiguity if we use y_{lm} or Y_{lm} in what follows.

The orthogonality of the spherical harmonics in $L^2(S)=L^2([0,\pi]\times[0,2\pi])$ with respect to $d\Omega=\sin\theta d\theta d\phi$ for different values of m is easily shown: it is sufficient to show that $e^{im\phi}$ are orthogonal on $[0,2\pi]$. The orthogonality of the spherical harmonics for different values of l can be derived from the fact that they are solutions to the eigenvalue-problem (7.6): $L^2Y_{lm}=\lambda Y_{lm}=l(l+1)Y_{lm}$. The operator L^2 (7.4) is self-adjoint: it is the negative Laplacian operator $-\nabla^2$ on the sphere S (7.3), that is $r=constant=1$; so the usual proof applies:

$$
l'(l'+1)<Y_{l'm'},Y_{lm}>=<L^2Y_{l'm'},Y_{lm}>=<Y_{l'm'},L^2Y_{lm}>=l(l+1)<Y_{l'm'},Y_{lm}>\,,
$$

and for $l'\neq l$ this equation can only be true if $<Y_{l'm'},Y_{lm}>=0$.

Rotations

The same type of operator technique can be used to prove ([Weissbluth, 78] page 57-58) that the spherical harmonics Y_{lm}, $m \in \{l, l-1, ..., 0, ..., -l+1, -l\}$ transform among themselves under rotations $\mathcal{R}_o$. We showed that the Laplacian operator ∇^2 and the rotation operator $\mathcal{R}_o$ commute: consider (6.10), therefore L^2 and $\mathcal{R}_o$ commute too, and we have:

$$L^2\mathcal{R}_o Y_{lm} = \mathcal{R}_o L^2 Y_{lm} = l(l+1)\mathcal{R}_o Y_{lm}\,,$$

that is $\mathcal{R}_o Y_{lm}$ is an eigenfunction of L^2 with eigenvalue $l(l+1)$. Now, since the only eigenfunctions of L^2 with eigenvalue $l(l+1)$ belongs to $span\,\{Y_{lm}\}_{m\in\{l,.....,-l\}}$ we conclude $\mathcal{R}_o Y_{lm} \in span\,\{Y_{lm}\}_{m\in\{l,.....,-l\}}$. We have proved the property (6.5) for the spherical harmonics y_{lm} and as a consequence also for the functions $T_{nl}y_{lm}$ used in the expansion (7.34) since the radial functions T_{nl} are independent of rotations.

Analytical expressions for the coefficients r_{lm} in $\mathcal{R}_o Y_{lm} = \sum_{m=-l}^{l} r_{lm} Y_{lm}$ exist, compare with (6.5), and they are used in Hex. The (lengthly) derivation of the coefficients is linked to the property of SO(3) being a subgroup of SU(2). Proofs can be found in [Weissbluth, 78] pages 100 -101, [Erdelyi et al, 53] pages 256-257 (maybe the most straightforward proof) and [Biedenharn and Louck, 81] page 47. In [Andrews et al, 99] pages 476-477 the relation of SO(3) to SU(2) is discussed, a discussion is also to be found in [Dieudonné, 80].

A proof of the completeness of the spherical harmonics can be found in [Erdelyi et al, 53] pages 241 (for continuous functions though but they form a dense subset of $L^2(S) = L^2([0,\pi]\times[0,2\pi])$). In our exposition we can refer to the self-adjointness of $L^2 = -\nabla^2$ on $L^2(S) = L^2([0,\pi]\times[0,2\pi])$ and spectral theory.

Translations

It is less obvious that the property (6.4) should be true for the functions $T_{nl}y_{lm}$, in fact it seems that this property only can be true, if possible at all ($\{T_{nl}y_{lm}\}_{nlm}$ do not form a complete set in $L^2(R^3)$), for an *infinite* summation. Ritchie and Kemp state the property ([Ritchie & Kemp, 00] page 180) but they do not use it, instead they consider the shape complementarity score S (6.1) and calculates numerically the integrals in S for different distances (along the z-axis) between the two proteins using a coordinate transformation to prolate spherical coordinates ([Ritchie, 98] page 120-123). Ritchie and Kemp give references to [Talman, 68] and [Danos & Maximon, 65]. In [Danos & Maximon, 65] they by Taylor's theorem consider the operator $e^{\mathbf{h}\cdot\nabla}$ (which somehow also is the approach in [Talman, 68]) and a *free field*, that is solutions to the wave equation $(\nabla^2 + k^2)\psi = 0$, k a number. Having the preceding proof of the property (6.5) in mind we note that the translation operator $\mathcal{T}_{\mathbf{r}_o}$ commute with ∇^2 and k^2. We also know that the functions $\{T_{nl}y_{lm}\}_{nlm}$typically are solutions to a kind [the type of the associated Laguerre polynomials is changed and they are scaled] of Schrödinger equation with a potential $V(r)$, that is, they are not free-field solutions and also, the translation operator $\mathcal{T}_{\mathbf{r}_o}$ and the potential $V(r)$ do not commute. It is not likely that the property (6.4) is true for the functions $T_{nl}y_{lm}$.

Chapter 8

Numerical Simulation

We now with the help of Matlab numerically investigate the radial functions S_{nl} and the expansion (7.34). A Matlab-code has been written and is attached as an appendix. The investigations are of course made under the presumption that our code is correct. A comparison with Ritchie's Ph.D. thesis is not immediately possible, since as mentioned above, apparently the applied functions have changed.

8.1 Surface shaped radial functions S_{nl}

We first want to plot the graphs of some of the functions S_{nl} (7.35). The Matlab-code uses the first associated Laguerre polynomials $L_0^\alpha(x) = 1$ and $L_1^\alpha(x) = \alpha + 1 - x$, and the following recurrence-relation ([Erdelyi et al, 53] page 188) for the associated Laguerre polynomials $L_n^\alpha(x)$:

$$(n+1)L_{n+1}^\alpha(x) - (2n + \alpha + 1 - x)L_n^\alpha(x) + (n+\alpha)L_{n-1}^\alpha(x) = 0\,.$$

l=0

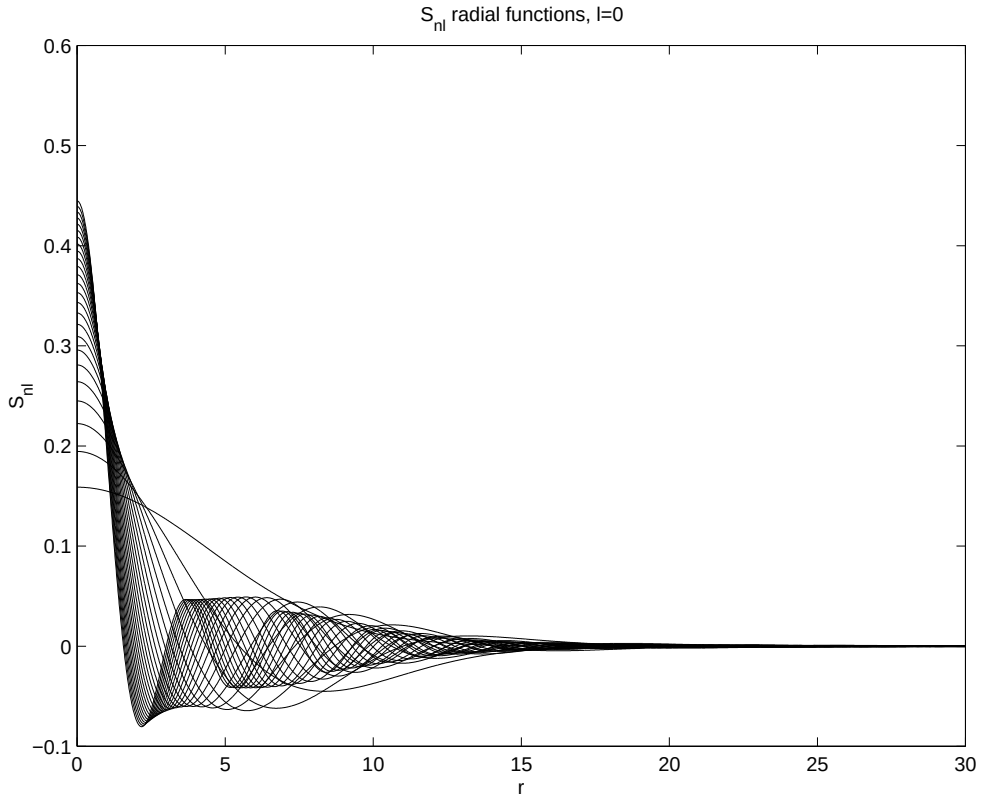

We see that the functions S_{n0} are almost zero for r larger than 15 (Å). The factor $e^{-\frac{\rho}{2}}$ makes the S_{nl} functions decay in competition with the factor $\rho^{\frac{l}{2}}$ which makes the functions grow.

l=10

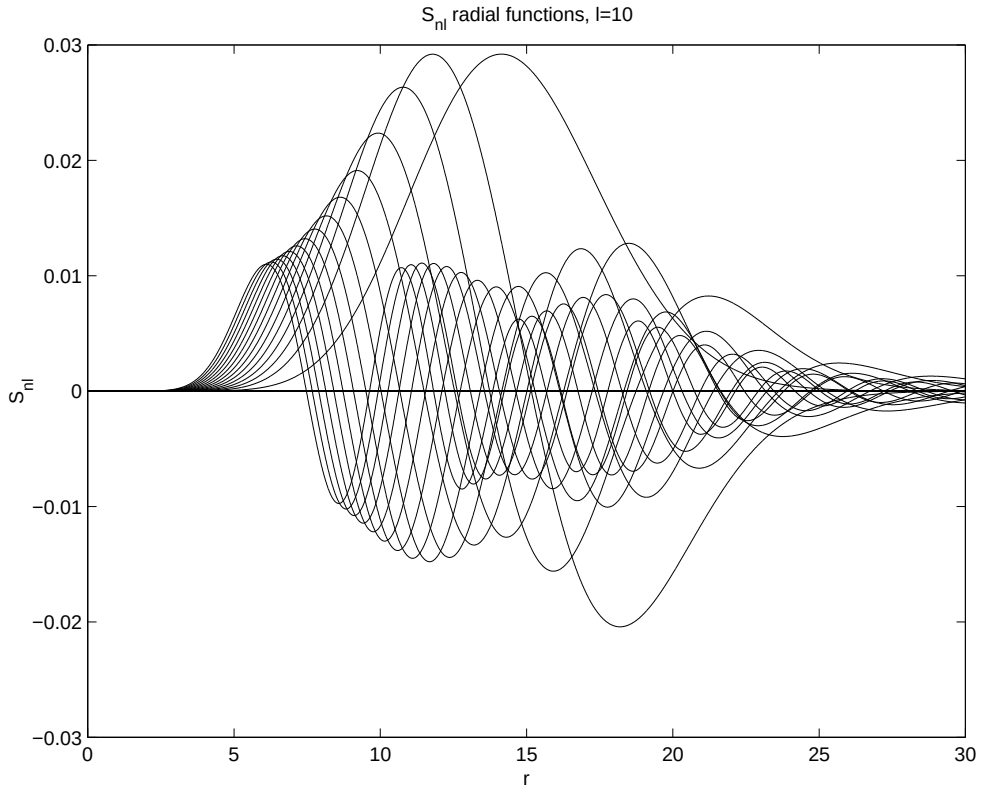

The S_{n10} functions "lives" in the interval 7-22. Presumably is this due to the factor $\rho^{\frac{l}{2}}$.

l=20

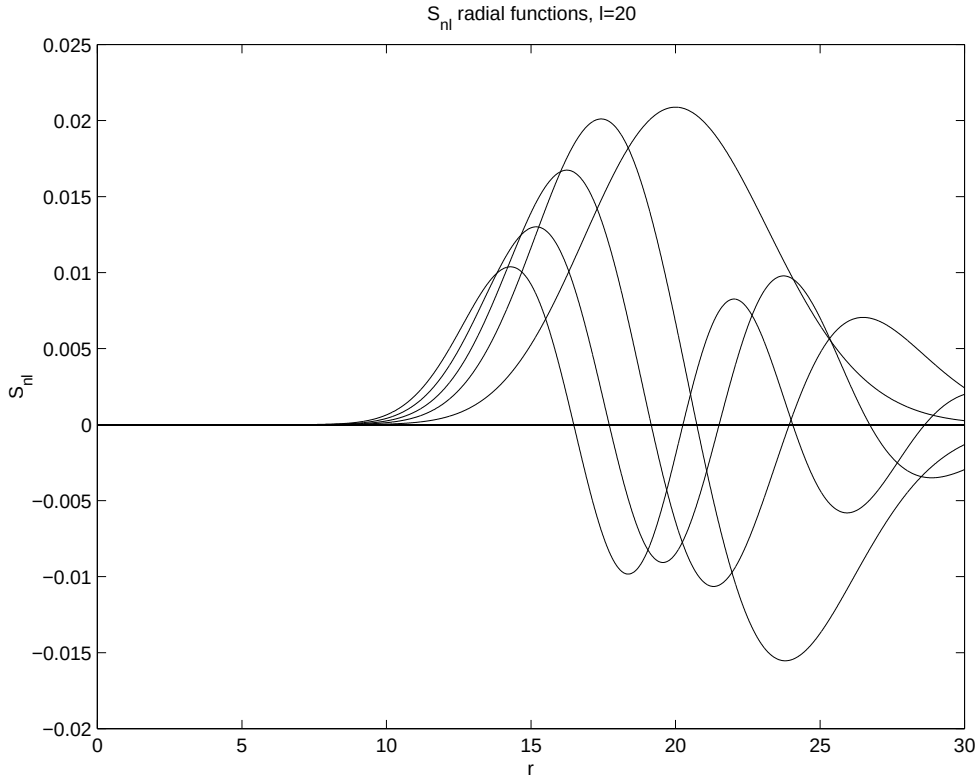

The functions S_{n20} "lives" in the interval 15-30.

As a first impression one could wonder if these functions can be used in the representation of the radial shape of proteins, but maybe the radials precisely are "tuned" to do that. For instance the spherical shape of a protein will be most predominant close to the center and considering the S_{n0} functions they "live" in the interval 0-15 (Å) close to the center.

8.2 Expansion

Next we want to make a simple analysis of how good the spherical expansion used in Hex is. We consider a shell σ between a sphere of radius r_1 and a sphere of radius r_2, where $r_1 < r_2$. The characteristic function f for the shell is

$$f(\mathbf{r}) = 1_\sigma(\mathbf{r}) = \begin{cases} 1 & for\, \mathbf{r} \in \sigma \\ 0 & for\, \mathbf{r} \notin \sigma \end{cases} ,$$

and in spherical coordinates we have

$$f(r,\theta,\phi) = 1_{[r_1,r_2]}(r) = \begin{cases} 1 & for\, r \in [r_1, r_2] \\ 0 & elsewhere \end{cases} .$$

This characteristic function is expanded to N'th order:

$$f_N(\mathbf{r}) = \sum_{nlm}^{N} a_{nlm} S_{nl}(r) y_{lm}(\theta,\phi) .$$

If we multiply with $S_{n'l'}y_{l'm'}$ in this equation (with f instead of f_N of course) and integrate we get due to the orthonormality of the $S_{nl}y_{lm}$-functions and because f is independent of θ and ϕ:

$$a_{nlm} = \int f(r,\theta,\phi)S_{nl}(r)y_{lm}(\theta,\phi)dV = \left(\int_0^\infty 1_{[r_1,r_2]}(r)S_{nl}(r)r^2dr\right)\left(\int y_{lm}(\theta,\phi)d\Omega\right) .$$

We can evaluate the integrals $\int y_{lm}(\theta,\phi)d\Omega$ ([Weissbluth, 78] page 11). We have the orthonormality property (7.32) $\int y_{lm}(\theta,\phi)y_{l'm'}d\Omega = \delta_{ll'}\delta_{mm'}$ and also $y_{00} = \frac{1}{\sqrt{4\pi}}$ (for instance use (7.31)) or $1 = \sqrt{4\pi}y_{oo}$, therefore

$$\int y_{lm}(\theta,\phi)d\Omega = \int \sqrt{4\pi}y_{oo}y_{lm}(\theta,\phi)d\Omega = \sqrt{4\pi}\delta_{l0}\delta_{m0} .$$

We conclude that only the coefficients a_{n00} are nonzero and equal to:

$$a_{n00} = \sqrt{4\pi}\int_{r_1}^{r_2} S_{nl}(r)r^2dr .$$

Using this result the Matlab-code gives the following results for thickness $r_2 - r_1 = 1.4$ (Hex uses surface skins of thickness 1.4Å), where we also have compared with a simple expansion in step-functions (called a Haar basis in [Goswami & Chan, 99] (page 13)).

Shell 8-9.4

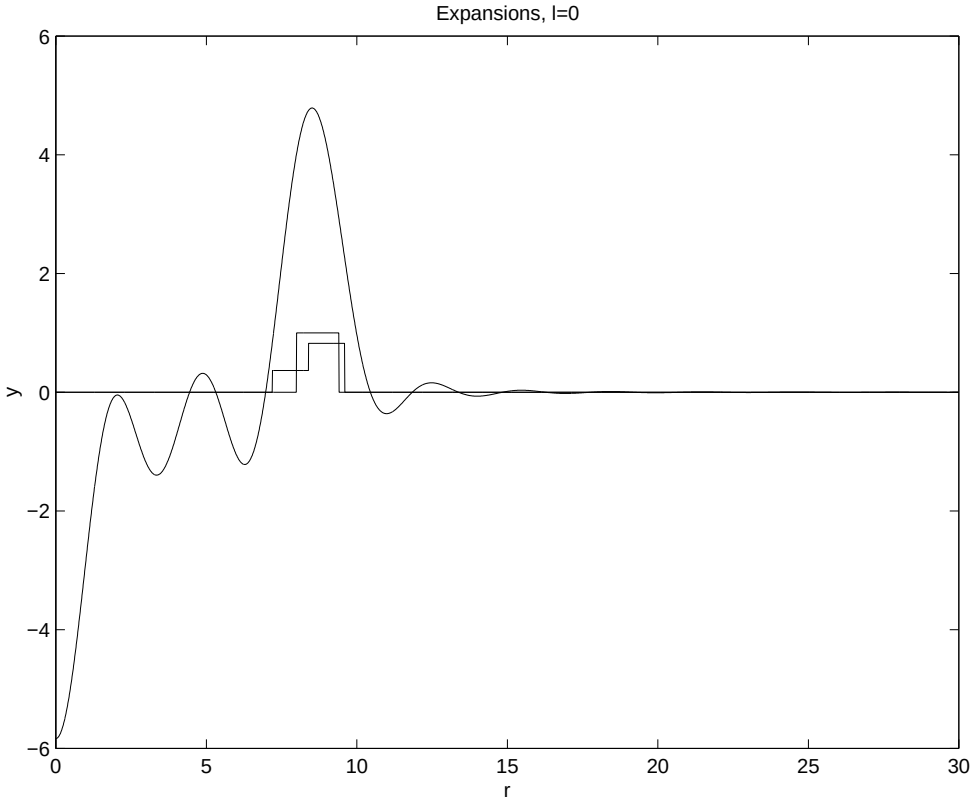

Clearly the expansion does represent the shell with radii in the interval 8Å-9.4Å as a "peak" but also a lot of "polynomial noise" is present, the "noise" should be compared with that ordinary Fourier expansions too do have some unwanted effects in representing step-functions: the phenomenon of Gibbs. The expansion in the Haar basis functions is better.

Shell 15-16.4

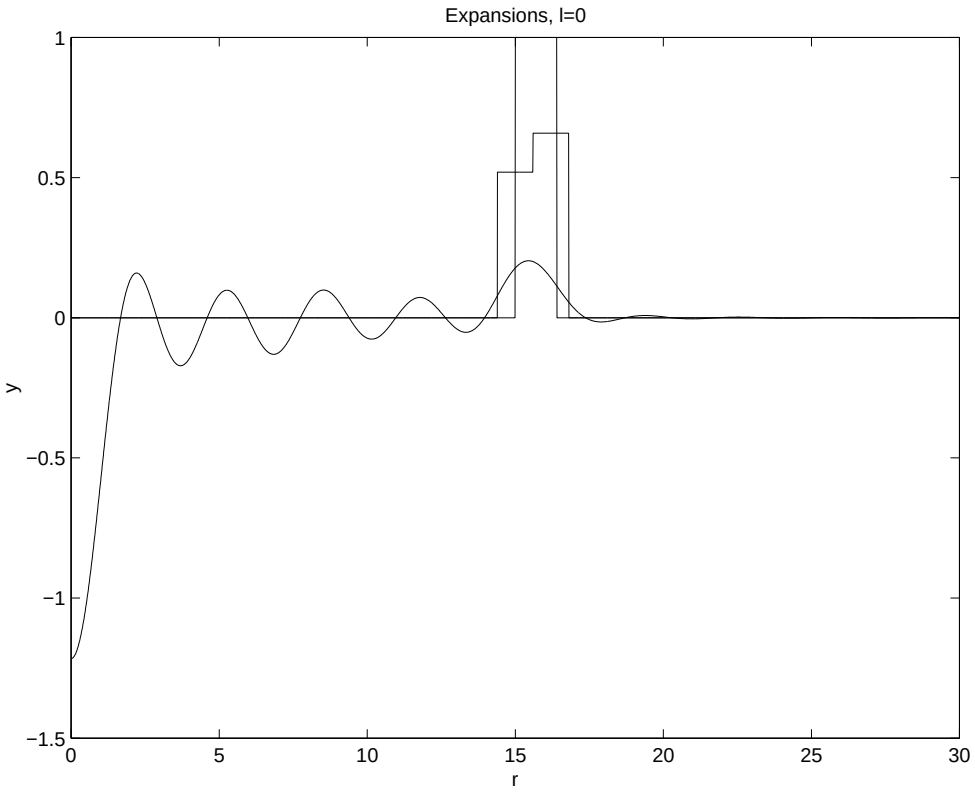

This time the "peak" again is located where it should but now clearly smaller. We can explain this as a consequence of that the functions S_{n0} essentially are zero for large values of r.

Part III

Discussion

Chapter 9

Discussion

We now try to discuss the preceding to see if we can draw any conclusions.

9.1 Solvent Effects

One could pose the question: how important are the solvent effects? According to the talk by Per Siegbahn November 7, 2002, at QUP on density functional calculations the effects in general are small; but Siegbahn also gave an example where the solvent or dielectric effects were important.

The biomolecule is in an dielectric cavity; do Cossi et al [Cossi et al, 02] use any differential geometric methods or tools? The answer is yes. The cavity surface is mapped with small elements called "tesserae", that is small tiles, making it possible to calculate surface integrals as finite sums. A polarization charge density $\sigma(\mathbf{s})$ is spread on the cavity surface and through a reaction field method solvent effects on energies in molecular mechanics can be calculated, while in quantum calculations the Hamiltonian is corrected by an appropriate operator. The computing procedure or code obtained is efficient.

The formulation of Cossi et al is implemented in development versions of the GAUSSIAN [Gaussian] package. The use of software packages in quantum chemistry is inevitable, and impressing results have been obtained (compare with [Pople, 99] and [Kohn, 99]) but to some extent, if one is trying to look for improvements, this maybe also makes the field less transparent.

9.2 Biomembranes

From the point of view of applications biomembranes probably are an interesting field; already the example of human red blood cells shows this.

It was very interesting to see an application of classical differential geometry on a problem from mathematical physics which not was the usual case of general relativity. The reference [Ou-Yang et al, 99] is well-provided with lengthly calculations, this is maybe a part of the game. If one has to do fast investigations it is recommended to use The

Surface Evolver [Evolver, 99]; in the reference [Ou-Yang et al, 99] some results are based on the use of The Surface Evolver. Apparently has the non-linear *general shape equation* (4.2) not been systematically studied, a subject for the energetic mathematician!

9.3 Docking Programs

As mentioned earlier The Cancer Research in the UK has a site on the Internet with links to some docking programs [smithgr, 02], more than ten programs are presented and reading the references in [Halperin et al, 02] carefully one would probably find a few more.

It must be stressed that docking depend on the case considered, large protein - large protein docking is not the same as protein - small biomolecule docking and the methods employed will somehow differ. For instance the article of Kuntz [Kuntz, 92] seems to be directed towards docking of small molecules, whereas the article of Ritchie and Kemp [Ritchie & Kemp, 00] more is directed towards docking of large proteins. The name "ligand" which Kuntz sets in quotation marks does in common usage in the first place refer to ions, atoms, or molecules surrounding a central atom ([Weissbluth, 78] page 650), but in docking terminology larger molecules can be named ligands too and they are considered to associate with not only single atoms but also larger molecules.

Kuntz tells how DOCK can be used to generate *leads* searching databases; in the final step the best ranking leads are viewed using computer-graphics. Of course docking programs have been improved since the arrival of DOCK but the problem of *false positives* has not been solved yet and will not be solved in a foreseeable future. The improvements of docking programs is probable to come in the field of *fast computation* with *reliable positives* and as *few false positives as possible* together with development of methods allowing *flexible* molecules.

9.3.1 Methods

A large number of different methods are used in docking procedures [Halperin et al, 02].

With respect to the general docking procedures or representations we saw, among the methods considered above, that the only program exploring the classical energy of the two molecules was DARWIN. The other programs employed geometric methods: DOCK used spheres, both the Fourier methods used surface skins, The Geometric Hashing Method used "knobs", "holes" and normals and finally BIGGER used a digital grid. BIGGER had implemented "soft belt" regions allowing penetration corresponding to typical changes in conformations; another way of introducing flexibility was the use of torsion angles as in FLEXE.

9.3.2 Hex

Maybe the most obvious geometrical idea of Hex is to exploit the spherical symmetry: an easy way to implement rotations will make the subsequent calculations easier. The idea of

only calculating the expansion coefficients once is also obvious. Using expansions further makes it possible to precalculate transformation coefficients. Whether the transformation coefficients can be calculated analytically or have to be calculated numerically and stored on disc for subsequent use is maybe not of vital importance with the standards of todays computers; Hex requires around 55 Mb of disc space storing integrals but todays personal computers are equipped with 256 Mb of RAM. We have not considered the many computational aspects of Hex but, Hex is fast: $6.3 \cdot 10^8$ translations and rotations in half an hour on a 1GHz Pentium III (from the reference manual of Hex); being so fast is to a high degree a consequence of these ideas.

One can question if the chosen spherical polar Fourier expansion is the right one, it apparently works well, but it is also well-known that Fourier expansions do have some unwanted effects in representing step-functions: the phenomenon of Gibbs. Ritchie and Kemp also say their method for calculating the electrostatic energy is not the best (page 185 in [Ritchie & Kemp, 00]) so improvements can be made, but the chosen procedure needs to be computationally fast.

9.3.3 Ideas for Improvements?

Consensus scoring as presented in [Halperin et al, 02] using different parameters such as for example statistics for amino acid contacts and hydrogen bonds is appealing, the problem though is that different parameters can require different representations slowing down the overall procedure.

An idea for improving the calculation of the electrostatical energy in Hex could be to investigate if the apparently fast method of Cossi et al [Cossi et al, 02] can be used in docking calculations. For the best ranking leads one could investigate if a fast, non-sophisticated code for density functional calculations can be developed (a monograph on density calculations is [Parr & Yang, 89]). If we again consider Hex an obvious idea would be to consider wavelets in the expansions; they are locally defined and the expansions are therefore easier to control. It is interesting to note that a theory for wavelets on the sphere exists: [Freeden & Schreiner, 98].

Appendix: Illustrations from Hex

The figures below are from the example-macro 2ptc.mac in the docking-program Hex (version 3.2).

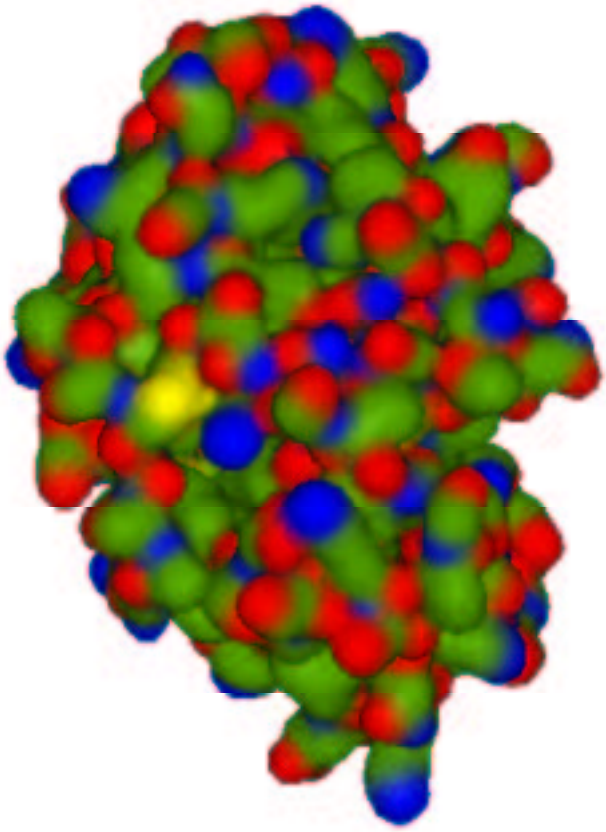

Receptor

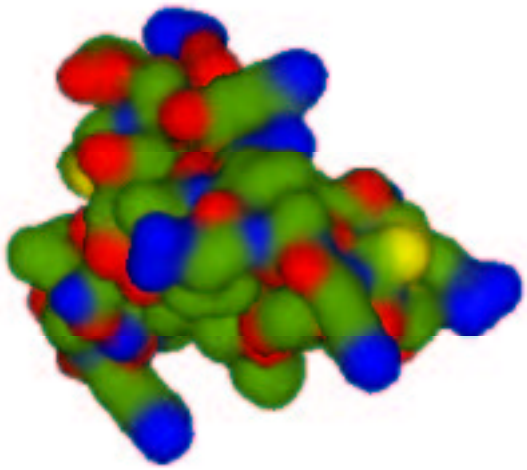

Ligand

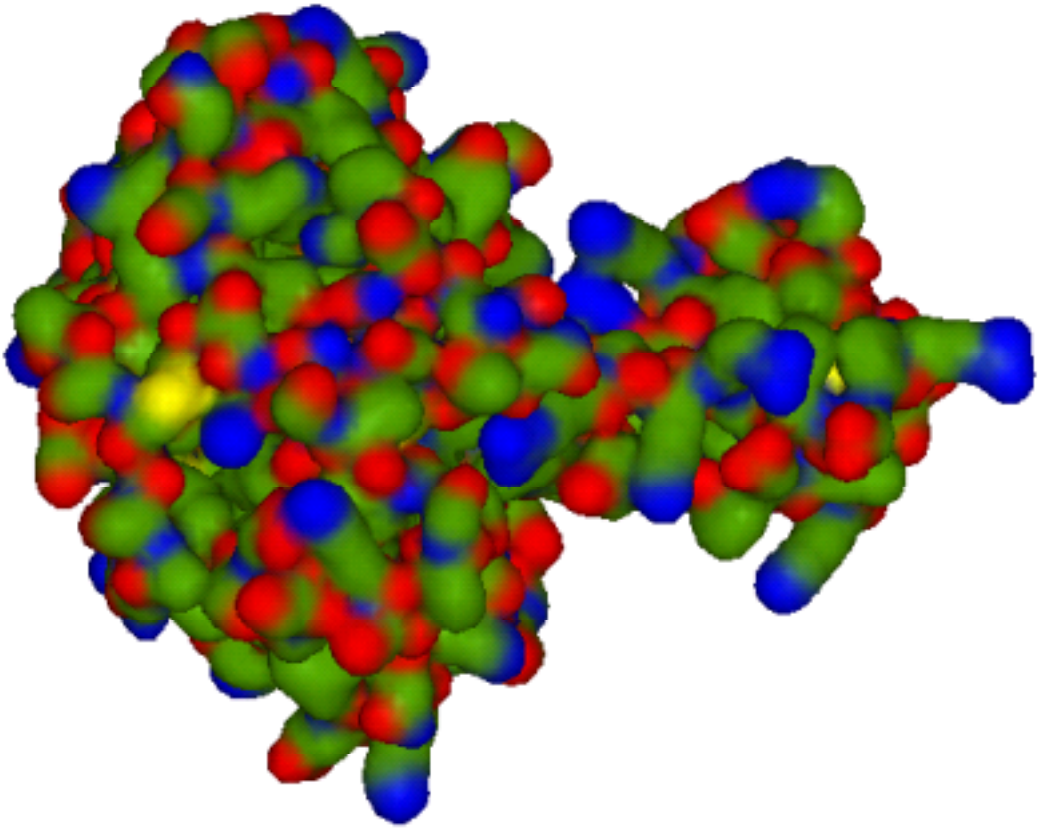

Docking: receptor and ligand associate.

Appendix: Matlab-code

```
%
%Protein Docking Using Spherical Polar Fourier Correlations
%Comparison of Laguerre- and Haar-type radial basis functions
%

%
%Initializations
%

clear all;
close all;
N=25;
dr=0.01;
r_end=30;
r=0:dr:r_end;
ONE=ones(1,length(r));

%
%Laguerre-type basis functions Snl of Ritchie and Kemp
%

l=20;
alpha=l+0.5;
k=20;
rho=r.^2/k;

Lalpha_rho=[];
Lalpha_rho(1,:)=ONE; %NOTE: this corresponds to n=0
Lalpha_rho(2,:)=(1+alpha)*ONE-rho; %n=1
for i=3:N
  Lalpha_rho(i,:)=((2*(i-1)+alpha+1)*ONE-rho).*Lalpha_rho(i-1,:)/i-(i-1+alpha)*Lalpha_rho(i-2,:)/i;
end

C=2^0.5/(k^0.75);

for i=(l+1):N
  Sl_r(i,:)=C*sqrt(prod(1:(i-l-1))/(pi^0.5*prod(0.5:1:(i-0.5))))*exp(-rho/2).*rho.^(l/2).*Lalpha_rho(i-
l,:);
end
```

```
%Note that the right Lalpha_rho is chosen due to their
%construction with the first corresponding to n=0

%plot(r,Sl_r)
%hold on

%
%Haar-type basis functions
%

Delta=r_end/N;
for i=1:N
phiH_r(i,:)=sqrt(3/((3*i^2-3*i+1)*Delta^3))*(((i-1)*Delta*ONE<=r)&(r<i*Delta*ONE));
end

%plot(r,phiH_r)
%hold on

%
%Skins
%

Skin1_r=(5*ONE<=r)&(r<=6.4*ONE);
Skin2_r=(15*ONE<=r)&(r<=16.4*ONE);

%plot(r,Skin1_r)
%hold on
plot(r,Skin2_r)
hold on

%
%Truncated expansion in Snl-functions
%

Skin1r2dr=Skin1_r.*r.^2*dr;
for i=(l+1):N
   a1(i)=sqrt(4*pi)*Sl_r(i,:)*Skin1r2dr';
end

Skin1NS_r=0*ONE;
for i=(l+1):N
   Skin1NS_r=Skin1NS_r+a1(i)*Sl_r(i,:);
end

%plot(r,Skin1NS_r)
%hold on


Skin2r2dr=Skin2_r.*r.^2*dr;
for i=(l+1):N
```

```
   a2(i)=sqrt(4*pi)*Sl_r(i,:)*Skin2r2dr';
end

Skin2NS_r=0*ONE;
for i=(l+1):N
   Skin2NS_r=Skin2NS_r+a2(i)*Sl_r(i,:);
end

plot(r,Skin2NS_r)
hold on


%
%Truncated expansion in phiH_r functions
%

for i=1:N
   b1(i)=phiH_r(i,:)*Skin1r2dr';
end

Skin1NH_r=0*ONE;
for i=1:N
   Skin1NH_r=Skin1NH_r+b1(i)*phiH_r(i,:);
end

%plot(r,Skin1NH_r)
%hold on


for i=1:N
   b2(i)=phiH_r(i,:)*Skin2r2dr';
end

Skin2NH_r=0*ONE;
for i=1:N
   Skin2NH_r=Skin2NH_r+b2(i)*phiH_r(i,:);
end

plot(r,Skin2NH_r)
hold on
```

List of Figures

Bibliography

[Jakubke & Jeschkeit, 82] Hans-Dieter Jakubke, Hans Jeschkeit: *Aminosäuren, Peptide, Proteine*. Akademie-Verlag, Berlin, 1982.

[Schulz & Schirmer, 79] Georg E. Schulz, R. Heiner Schirmer: *Principles of Protein Structure*. Springer-Verlag, New York, 1979.

[Branden & Tooze, 99] Carl Branden, John Tooze: *Introduction to Protein Structure*. Garland Publishing, New York, 1999.

[Stryer, 88] Lubert Stryer: *Biochemistry*. W. H. Freeman and Company, New York, 1988.

[Ou-Yang et al, 99] Ou-Yang Zhong-Can, Liu Ji-Xing and Xie Yu-Zhang: *Geometric Methods in the Elastic Theory of Membranes in Liquid Crystal Phases*. World Scientific, Singapore, 1999.

[Pople, 99] John A. Pople: Nobel Lecture: Quantum chemical models. Rev. Mod. Phys., Vol. 71, No. 5, p. 1267-1273, October 1999.

[Kohn, 99] W. Kohn: Nobel Lecture: Electronic structure of matter - wave functions and density functionals. Rev. Mod. Phys., Vol. 71, No. 5, p. 1253-1266, October 1999.

[Gaussian] The Gaussian package: *Gaussian, Inc., Carnegie Office Park, Building 6, Pittsburgh, PA 15106 U.S.A.*

[Jensen, 98] Frank Jensen: *Introduction to Computational Chemistry*. John Wiley & Sons, Chichester, 1998.

[Brooks et al, 83] Bernard R. Brooks, Robert E. Bruccoleri, Barry D. Olafson, David J. States, S. Swaminathan and Martin Karplus, CHARMM: A Program for Macromolecular Energy, Minimization, and Dynamics Calculations. Journal of Computational Chemistry, Vol. 4, No. 2, 187-217 (1983).

[antas] See the Internet site: http://antas.agraria.uniss.it/software.html#

[Foresman et al, 96] James B. Foresman, Todd A. Keith, Kenneth B. Wiberg, John Snoonian and Michael J. Frisch: Solvent Effects. 5. Influence of Cavity Shape, Truncation of Electrostatics, and Electron Correlation on ab Initio Reaction Field Calculations. J. Phys. Chem. 1996, 100, 16098-16104.

[Onsager, 36] L. Onsager, J. Am. Chem. Soc., 1936, 58, 1486.

[Cossi et al, 02] Maurizio Cossi, Giovanni Scalmani, Nadia Rega and Vincenzo Barone: New developments in the polarizable continuum model for quantum mechanical and classical calculations on molecules in solution. J. Chem. Phys., 2002, Vol. 117, No. 1, page 43-54.

[Gordon et al, 01] Mark S. Gordon, Mark A. Freitag, Pradipta Bandyopadhyay, Jan H. Jensen, Visvaldas Kairys and Walter J. Stevens: The Effective Fragment Potential Method: A QM-Based MM Approach to Modeling Environmental Effects in Chemistry. J. Phys. Chem. A, Vol. 105, No. 2, 2001.

[Bandyopadhyay, 02] Pradipta Bandyopadhyay, Mark S. Gordon, Benedetta Mennucci and Jacopo Tomasi: An integrated effective fragment - polarizable continuum approach to solvation: Theory and application to glycine. J. Chem. Phys., Vol 116, No 12, page 5023-5032, 2002.

[Talpaert, 01] Yves Talpaert: *Differential Geometry with Applications to Mechanics and Physics*. Marcel Dekker, New York, 2001.

[Spiegel, 59] Murray R. Spiegel: *Vector Analysis and an Introduction to Tensor Analysis*. Schaum's Outline Series a McGraw-Hill Book Company, New York, 1959.

[Do Carmo, 76] Manfredo P. do Carmo: *Differential Geometry of Curves and Surfaces*. Prentice-Hall, New Jersey, 1976.

[Brakke, 92] K. Brakke, Exp. Math. 1 (1992), 141.

[Evolver, 99] K. Brakke, The Surface Evolver: http://www.susqu.edu/facstaff/b/brakke/evolver/evolver.htm

[Halperin et al, 02] Inbal Halperin, Buyong Ma, Haim Wolfson, and Ruth Nussinov: Principles of Docking: An Overview of Search Algorithms and a Guide to Scoring Functions. Proteins: Structure, Function, and Genetics 47: 409-443 (2002).

[Kuntz, 92] Irwin D. Kuntz: Structure-Based Strategies for Drug Design and Discovery. Science 257: 1078-1082 (1992).

[Connolly, 96] Michael L. Connolly: Molecular Surfaces: A Review. http://www.netsci.org/Science/Compchem/feature14.html, copyright date: 1996.

[Ritchie & Kemp, 99] David W. Ritchie and Graham J. L. Kemp: Fast Computation, Rotation, and Comparison of Low Resolution Spherical Harmonic Molecular Surfaces. Journal of Computational Chemistry, Vol. 20, No. 4, 383-395 (1999).

[Ritchie & Kemp, 00] David W. Ritchie and Graham J. L. Kemp: Protein Docking Using Spherical Polar Fourier Correlations. Proteins: Structure, Function, and Genetics 39: 178-194 (2000). The program Hex is available from its' Home Page: www.biochem.abdn.ac.uk/hex/

[Katchalski-Katzir et al, 92] Ephraim Katchalski-Katzir, Isaac Shariv, Miriam Eisenstein, Asher A. Friesem, Claude Aflalo, and Ilya A. Vakser: Molecular surface recognition: Determination of geometric fit between proteins and their ligands by correlation techniques. Proc. Natl. Acad. Sci. USA: Vol. 89, pp. 2195-2199, March 1992.

[smithgr, 02] Cancer Research UK, BioMolecular Modelling: http://www.bmm.icnet.uk/~smithgr/soft.html

[Norel et al, A, 94] Raquel Norel, Shuo L. Lin, Haim J. Wolfson, and Ruth Nussinov: Shape Complementarity at Protein-Protein Interfaces. Biopolymers, Vol. 34, 933-940 (1994).

[Norel et al, B, 94] Raquel Norel, Daniel Fischer, Haim J. Wolfson and Ruth Nussinov: Molecular surface recognition by a computer vision-based technique. Protein Engineering vol. 7 no. 1 pp. 39-46, 1994.

[Fisher et al, 95] Daniel Fischer, Shuo Liang Lin, Haim L. Wolfson and Ruth Nussinov: A Geometry-based Suite of Molecular Docking Processes. J. Mol. Biol. (1995) 248, 459-477.

[Palma et al, 00] P. Nuno Palma, Ludwig Krippahl, John E. Wampler, and José J.G. Moura: BIGGER: A New (Soft) Docking Algorithm for Predicting Protein Interactions. Proteins: Structure, Function, and Genetics 39: 372-384 (2000).

[Claußen et al, 01] Holger Claußen, Christian Buning, Matthias Rarey and Thomas Lengauer: FLEXE: Efficient Molecular Docking Considering Protein Structure Variations. J. Mol. Biol. (2001) 308, 377-395.

[Taylor & Burnett, 00] Jeffrey S. Taylor and Roger M. Burnett: DARWIN: A Program for Docking Flexible Molecules. Proteins: Structure, Function, and Genetics 41: 173-191 (2000).

[Rudin, 89] Walter Rudin: *Functional Analysis.* Tata McGraw-Hill Publishing Company Ltd., New Delhi, 13th reprint, 1989.

[Erdelyi et al, 53] Arthur Erdélyi, Wilhelm Magnus, Fritz Oberhettinger and Francesco G. Tricomi: *Higher Transcendental Functions, Volume II.* McGraw-Hill Book Company, New York, 1953.

[Birkhoff & Rota, 89] Garret Birkhoff and Gian-Carlo Rota: *Ordinary Differential Equations, Fourth Edition.* John Wiley & Sons, New York, 1989.

[Hinton & Schaefer, 97] Don Hinton and Philip W. Schaefer (editors): *Spectral Theory and Computational methods of Sturm-Liouville Problems.* Marcel Dekker, New York, 1997.

[Andrews et al, 99] George E. Andrews, Richard Askey and Ranjan Roy: *Special Functions.* Cambridge University Press, Cambridge, UK, 1999.

[Biedenharn and Louck, 81] Lawrence C. Biedenharn and James D. Louck: *Angular Momentum in Quantum Physics: Theory and Application.* Addison-Wesley, Reading, Massachusetts, USA, 1981.

[Dieudonné, 80] Jean Dieudonné: *Special Functions and Linear Representations of Lie Groups.* American Mathematical Society, Providence, Rhode Island, USA, 1980.

[Weissbluth, 78] Mitchel Weissbluth: *Atoms and Molecules, Student Edition.* Academic Press, San Diego, USA, 1978.

[Kristensen, 84] P. Kristensen: *Atomfysik og kvantemekanik.* Noter, Det Fysiske Institut, Aarhus Universitet, 1984/85.

[Talman, 68] James D. Talman: *Special Functions, A Group Theoretic Approach.* W. A. Benjamin, 1968.

[Danos & Maximon, 65] M. Danos & L. C. Maximon: Multipole Matrix Elements of the Translation Operator. Journal of Mathematical Physics, Volume 6, Number 5, May 1965.

[Ritchie, 98] David W. Ritchie: Parametric Protein Shape Recognition, Ph.D. thesis, Departments of Computing Science & Molecular and Cell Biology, University of Aberdeen, 1998. Available from David W. Ritchie's Home Page: www.csd.abdn.ac.uk/~dritchie/

[Hobson, 31] E. W. Hobson: *The Theory of Spherical and Ellipsoidal Harmonics*. London: Cambridge University Press, 1931.

[Pauling & Wilson, 35] L. Pauling & E. B. Wilson: *Introduction to Quantum Mechanics*. McGraw-Hill, New York, 1935.

[Goswami & Chan, 99] Jaidewa C. Goswami & Andrew K. Chan: *Fundamentals of Wavelets. Theory, Algorithms, and Applications*. John Wiley & Sons, New York, 1999.

[Parr & Yang, 89] Robert G. Parr & Weitao Yang: *Density-Functional Theory of Atoms and Molecules*. Oxford University Press, New York, 1989.

[Freeden & Schreiner, 98] W. Freeden & M. Schreiner: Orthogonal and Nonorthogonal Multiresolution Analysis, Scale Discrete and Exact Fully Discrete Wavelet Transform on the Sphere. Constructive Approximation (1998) 14: 493-515.